

AVERAGE VECTOR FIELD METHOD FOR HAMILTONIAN SYSTEMS

A THESIS SUBMITTED TO
THE GRADUATE SCHOOL OF NATURAL AND APPLIED SCIENCES
OF
ATILIM UNIVERSITY

BY

BAHAA AHMED KHALAF SABAWE

IN PARTIAL FULFILLMENT OF THE REQUIREMENTS
FOR
THE DEGREE OF MASTER OF SCIENCE
IN
MATHEMATICS

SEPTEMBER 2021

Approval of the Graduate School of Natural and Applied Sciences, Atılım University.

Prof. Dr. Ender Keskinliç
Director

I certify that this thesis satisfies all the requirements as a thesis for the degree of **Master of Science in Mathematics Department, Atılım University.**

Prof. Dr. Ayhan Aydın
Head of Department

This is to certify that we have read the thesis **AVERAGE VECTOR FIELD METHOD FOR HAMILTONIAN SYSTEMS** submitted by **BAHAA AHMED KHALAF SABAWE** and that in our opinion it is fully adequate, in scope and quality, as a thesis for the degree of Master of Science.

Prof. Dr. Ayhan Aydın
Supervisor

Examining Committee Members:

Prof. Dr. Tanıl Ergenç
Mathematics Department, Atılım University

Prof. Dr. Ayhan Aydın
Mathematics Department, Atılım University

Assoc. Prof. Dr. Canan Köroğlu
Mathematics Department, Hacettepe University

Date: September 27, 2021



I declare and guarantee that all data, knowledge and information in this document has been obtained, processed and presented in accordance with academic rules and ethical conduct. Based on these rules and conduct, I have fully cited and referenced all material and results that are not original to this work.

Name, Last Name : BAHAA AHMED KHALAF SABAWE

Signature :

ABSTRACT

AVERAGE VECTOR FIELD METHOD FOR HAMILTONIAN SYSTEMS

Sabawe, Bahaa Ahmed Khalaf

M.S., Department of Mathematics

Supervisor : Prof. Dr. Ayhan Aydın

September 2021, 59 pages

In this thesis, we present and analyze four energy preserving methods for the numerical solution of initial value problems of Hamiltonian type. In particular, the average vector field (AVF) and partitioned AVF (PAVF) methods are used to drive energy preserving methods. In addition to these two energy preserving methods, two energy persevering PAVF composition (PAVF-C) and PAVF plus (AVF-P) methods are presented. The thesis accompanied numerical result for Zakharov system that demonstrate remarkable properties of the proposed energy persevering methods. In this thesis, this is the first time that energy persevering AVF, PAVF, PAVF-C and PAVF-P methods are proposed for Zakharov system. It is shown that PAVF and PAVF-C methods for Zakharov system are linearly implicit methods that have remarkable lower cost than the original AVF method. In addition, we further show that the PAVF methods preserve the mass conservation of the Zakharov system while the AVF method cannot.

Keywords: Hamiltonian systems, Average Vector Field Method, Partitioned Average Vector Field Method, Zakharov equation

ÖZ

HAMILTON SİSTEMLER İÇİN ORTALAMA VEKTÖR ALANI METODU

Sabawe, Bahaa Ahmed Khalaf

Yüksek Lisans,

Tez Yöneticisi : Prof. Dr. Ayhan Aydın

Eylül 2021, 59 sayfa

Bu tez çalışmasında Hamilton tipindeki başlangıç değer problemlerinin sayısal çözümü için enerji koruyan yöntemler ortaya konulmuş ve analiz edilmiştir. Özel olarak, enerji koruyan yöntemler olarak bilinen ortalama vektör alanı (AVF) ve bölmeli AVF (PAVF) yöntemleri kullanılmıştır. Bunlara ek olarak enerji koruyan birleşim (PAVF-C) yöntemi ve toplam (PAVF-P) yöntemleri kullanılmıştır. Bu tez çalışmasında bahsi geçen enerji koruyan yöntemlerin performanslarını ölçmek için Zakharov sistemi ele alınmıştır. Bu tez ile ilk olarak Zakharov sistemi için enerji koruyan AVF, PAVF, PAVF-C ve PAVF-P yöntemleri oluşturulmuştur. Zakharov sisteminin sayısal çözümünde linear kapalı yöntemler oluşları sebebiyle PAVF ve PAVF-C yöntemlerinin, AVF yöntemine göre kayda değer daha az sürede sonuç verdiği gösterilmiştir. Ayrıca, PAVF metodunun AVF metodunun aksine Zakharov sisteminin kütle korunumunu da koruduğu gösterilmiştir.

Anahtar Kelimeler: Hamilton sistemler, Ortalama Vektör Alanı, Bölmeli Ortalama Vektör Alanı, Zakharov denklemi



To Father & Mother

ACKNOWLEDGMENTS

First, I would like to express my deepest gratitude to my supervisor Prof. Dr. Ayhan Aydın, who was as father with me; thanks for his time, knowledge and effort . Second, I would like to express my gratitude to Prof. Dr. İnci Erhan for her , time and advices. I can't only be thankful and great full to her. Also, I would like to thank my family for their endless love and support that they provided for me in all the stages of my life. Finally, I would like to present all of my gratitude to all the teachers in the Department of Mathematics, Atılım University and my colleagues.

TABLE OF CONTENTS

ABSTRACT	iii
ÖZ	iv
DEDICATION	v
ACKNOWLEDGMENTS	vi
TABLE OF CONTENTS	vii
LIST OF TABLES	ix
LIST OF FIGURES	x
LIST OF SYMBOLS	xii
CHAPTERS	
1 INTRODUCTION	1
1.1 The Existence and Uniqueness of Solutions	1
1.2 One-step methods	3
1.2.1 Runge-Kutta Methods	5
1.3 Adjoint method and Composition method	7
2 HAMILTONIAN ORDINARY DIFFERENTIAL EQUATIONS	9
2.1 Hamiltonian Systems	10
2.2 The Average Vector Field Method	13
2.3 The Partitioned Average Vector Field Method	15
2.4 Numerical example	17
2.4.1 Hénon-Heiles System	18
3 HAMILTONIAN PARTIAL DIFFERENTIAL EQUATIONS	25
3.1 Inroduction	25

3.2	The nonlinear Schrödinger Equation	26
3.3	The good Boussinesq equation	28
3.4	Klein-Gordon Schrödinger Equation	29
3.4.1	Energy preserving AVF and PAVF schemes for Klein-Gordon Schrödinger equation	30
3.5	Zakharov System	34
3.5.1	Energy preserving AVF and PAVF schemes for Zakharov system	35
3.5.2	Numerical Experiments	38
3.5.2.1	Evolution of single soliton	42
3.5.2.2	Colliding solitons	47
4	CONCLUSION	55
	REFERENCES	56

LIST OF TABLES

TABLES

Table 3.1	Temporal accuracy for the energy preserving AVF method with $T = 10$ and $N = 256$	40
Table 3.2	Temporal accuracy for the energy and the mass preserving PAVF method with $T = 10$ and $N = 256$	40
Table 3.3	Temporal accuracy for the energy and the mass preserving PAVF-C method with $T = 10$ and $N = 256$	40
Table 3.4	Temporal accuracy for the energy and the mass preserving PAVF-P method with $T = 10$ and $N = 256$	41
Table 3.5	Spatial accuracy for the energy preserving PAVF method with $\Delta t = 0.01$	41
Table 3.6	Spatial accuracy for the energy and the mass preserving PAVF method with $\Delta t = 0.01$	41
Table 3.7	Spatial accuracy for the energy and the mass preserving PAVF-C method with $\Delta t = 0.01$	41
Table 3.8	Spatial accuracy for the energy and the mass preserving PAVF-P method with $\Delta t = 0.01$	42
Table 3.9	Computational costs of one soliton solution by energy preserving schemes with $\tau = 0.01$ at $T = 1$	47

LIST OF FIGURES

FIGURES

Figure 2.1 A simple harmonic oscillator in classical mechanics is a particle which is acted upon by a restoring force proportional to its displacement from its equilibrium position.	11
Figure 2.2 Chaotic orbit of the four energy preserving methods for the Henon Heiles system till $T = 2000$. (a) The AVF method, (b) The PAVF method, (c) The PAVF-C method, (d) The PAVF-P method.	21
Figure 2.3 Relative errors in energy (2.39) of the four energy preserving methods for the Henon Heiles system till $T = 2000$. (a) The AVF method, (b) The PAVF method, (c) The PAVF-C method, (d) The PAVF-P method.	22
Figure 2.4 Box orbit of the four energy preserving methods for the Henon Heiles system till $T = 1000$. (a) The AVF method, (b) The PAVF method, (c) The PAVF-C method, (d) The PAVF-P method.	23
Figure 2.5 Relative errors in energy (2.39) of the four energy preserving methods for the Henon Heiles system till $T = 1000$. (a) The AVF method, (b) The PAVF method, (c) The PAVF-C method, (d) The PAVF-P method.	24
Figure 3.1 Propagation of one soliton: $ \phi(t, x) $	43
Figure 3.2 Propagation of one soliton: $\psi(t, x)$	43
Figure 3.3 Relative Hamilton error for the propagation of one soliton: $ \phi(t, x) $	44
Figure 3.4 Relative norm error for the propagation of one soliton: $\psi(t, x)$	44
Figure 3.5 Propagation of one soliton: $ \phi(t, x) $	45
Figure 3.6 Propagation of one soliton $\psi(t, x)$	46
Figure 3.7 Relative Hamiltonian error for the propagation of one soliton.	46
Figure 3.8 Relative norm error for the propagation of one soliton.	47

Figure 3.9 The head-on collision of two solitary waves. AVF scheme.	49
Figure 3.10 The head-on collision of two solitary waves. PAVF scheme.	50
Figure 3.11 The head-on collision of two solitary waves. PAVF-C scheme.	51
Figure 3.12 The head-on collision of two solitary waves. PAVF-P scheme.	52
Figure 3.13 The head-on collision of two solitary waves. Profile of $ \phi(t, x) $	53
Figure 3.14 The head-on collision of two solitary waves. Profile of $\psi(t, x)$	53
Figure 3.15 The head-on collision of two solitary waves. Relative Hamiltonian errors.	54
Figure 3.16 The head-on collision of two solitary waves. Relative norm errors.	54



LIST OF SYMBOLS

- \mathbb{N} : the set of natural numbers
- \mathbb{N}_0 : the set of non-negative integers
- \mathbb{Z} : the set of integers
- \mathbb{R} : the set of real numbers
- \mathbb{R}^n : the n -dimensional real space
- $\langle x, y \rangle$: standard inner product of the vectors $x, y \in \mathbb{R}^n$
- ∇ : Gradient operator

CHAPTER 1

INTRODUCTION

In this chapter, we introduce basic definitions and notation used throughout the thesis. Additional notation will be introduced in specific sections as it is needed. Moreover a brief introduction for numerical methods for the initial-value problem is discussed.

1.1 The Existence and Uniqueness of Solutions

An Initial Value Problem (IVP) consists of a first-order differential equation and an initial condition of the form

$$\begin{aligned}\frac{dy}{dt} &= f(t, y(t)) \\ y(t_0) &= y_0.\end{aligned}\tag{1.1}$$

Solution of the IVP (1.1) is a function $y = \phi(t)$ satisfying the differential equation $\frac{dy}{dt} = f(t, y(t))$ and initial condition $y(t_0) = y_0$. For example, the analytic solution of the IVP

$$\begin{aligned}\frac{dy}{dt} &= 2y \\ y(0) &= 3\end{aligned}\tag{1.2}$$

is

$$\phi(t) = 3e^{2t}.$$

Unfortunately, not every IVP of the form (1.1) has an analytic solution. Some assumptions must be made about $f(t, y(t))$, and even then we can find the solution in a neighbourhood of $t = t_0$.

Theorem 1.1.1 *Consider the IVP (1.1). If f is continuous in a rectangle R centered*

at (t_0, u_0) , say

$$R = \{(t, y) : |t - t_0| \leq \alpha, |y - y_0| \leq \beta, \} \quad (1.3)$$

then the IVP (1.1) has a solution $y = \phi(t)$ for $|t - t_0| \leq \min(\alpha, \beta/M)$, where M is the maximum of $|f(t, y(t))|$ in the rectangle R .

Even if f is continuous, that the IVP (1.1) may not have a unique solution. For example, the IVP

$$\frac{dy}{dt} = y^{2/3}, \quad y(0) = 0 \quad (1.4)$$

has a solution $y(t) = 0$. Another solution is the function $y(t) = t^3/27$. To prove that the IVP (1.1) has unique solution, it is necessary to assume somewhat more about f .

Theorem 1.1.2 *If f and $\frac{\partial f}{\partial y}$ are continuous in the rectangle R defined by (1.3), then the IVP (1.1) has a unique solution in the interval $|t - t_0| < \min(\alpha, \beta/M)$.*

Note that $\partial f/\partial y = \frac{2}{3y^{1/3}}$ in (1.4) is not continuous at $t = 0$, hence f does not satisfy the hypothesis of the Theorem (1.1.2).

For many differential equations, it may not possible to find an analytical solution. For example, $dy/dt = t^2 + y^2$ has no analytical solution. If analytic solution are not available, numerical methods are relied upon to obtain an approximation. This process is called numerical integration, and the basic approach is to subdivide the time interval of integration $[t_0, t_f]$ into a collection of mesh points $\{t_0 < t_1 < \dots < t_n = t_f\}$ where $t_n = t_0 + nh$ for $n = 0, 1, \dots, N$. Here $N \in \mathbb{Z}^+$ and $h = \frac{1}{N}(t_f - t_0)$ is called the step-size of integration. Then, the exact solution $y(t_n)$ is approximated by y_n which is specified by the particular numerical method. The values y_n are calculated successively for $n = 1, \dots, N$. We will only consider methods in which h is held constant along the interval of integration.

In this thesis, we will consider only a one-step method which uses only one previous value, namely the Average Vector Field (AVF) method.

1.2 One-step methods

In this section we introduce one-step method. Before giving the general form of one-step method, first we consider the Euler method as an example. Explicit (or Forward) Euler's, or simply Euler's, method for a solution of the IVP (1.1) is given by

$$\begin{aligned} y_{n+1} &= y_n + hf(t_n, y_n), & n = 0, 1, 2, \dots, N-1 \\ y(t_0) &= y_0. \end{aligned} \quad (1.5)$$

The derivation of the Euler's method is straightforward. By the Taylor expansion of y about t_n , we have

$$\begin{aligned} y(t_{n+1}) &= y(t_n) + hy'(t_n) + \frac{h^2}{2!}y''(\hat{t}_n) + \mathcal{O}(h^3) \\ &= y(t_n) + hf(t_n, y_n) + \frac{h^2}{2!}y''(\hat{t}_n) + \mathcal{O}(h^3) \end{aligned}$$

where \hat{t}_n is a point in the interval (t_n, t_{n+1}) . Here, we assume that all derivatives of f do exist. Let y_n denotes the approximation to the true solution $y(t_n)$. If y'' is bounded and the step size h is small, we may ignore the last terms and write

$$y(t_{n+1}) \approx y_{n+1} = y(t_n) + hf(t_n, y_n).$$

which is the basis for (1.5). The repeated use of Euler's method for $n = 0, 1, 2, \dots$ produces the approximate solution y_1, y_2, y_3, \dots at the discrete points t_1, t_2, t_3, \dots . Euler's method is an explicit method since we can get the unknown y_{n+1} from the previous known approximation y_n , i.e. all information to find the next approximation is known. If the equation (1.1) is autonomous then Euler's method is simplified to

$$y_{n+1} = y_n + hf(y_n), \quad n = 0, 1, 2, \dots, N-1. \quad (1.6)$$

It is a one-step method since only one previous value is needed to determine the current value. A one-step method can be written in the general form

$$y_{n+1} = \phi_h(y_n) \quad (1.7)$$

for some suitable function ϕ . In the case of Euler's method $\phi_h(y_n) = y_n + hf(t_n, y_n)$. The implicit Euler method is same of the explicit Euler method, except that the function is evaluated at the value that is trying to estimate.

The implicit (or backward) Euler for (1.1) is,

$$\begin{aligned} y_{n+1} &= y_n + hf(t_{n+1}, y_{n+1}), & n = 0, 1, 2, \dots, N-1 \\ y(t_0) &= y_0. \end{aligned} \quad (1.8)$$

In (1.8), note that the approximation y_{n+1} is defined implicitly, which means that the unknown y_{n+1} on the left-hand-side depends on the unknown y_{n+1} and can not be solve explicitly in terms of the previous known values. Implicit methods are usually a nonlinear equation which must be solved to get the approximation y_{n+1} . Therefore, implicit methods require solving a system of nonlinear equations using numerical methods such as Newton-Raphson method.

The trapezoidal Rule for the numerical solution of (1.1)

$$y_{n+1} = y_n + h \frac{f(t_n, y_n) + f(t_{n+1}, y_{n+1})}{2} \quad (1.9)$$

is another one-step implicit method which averages the function evaluations at the past y_n and present y_{n+1} values.

The implicit midpoint rule for (1.1)

$$y_{n+1} = y_n + hf \left(\frac{t_n + t_{n+1}}{2}, \frac{y_n + y_{n+1}}{2} \right) \quad (1.10)$$

takes the function's estimation and averages it over the prior y_n and existing y_{n+1} values.

We must be aware of different types of errors when using a numerical method. Two types of error that are common in numerical calculations namely round-off error and truncation error. Round-off error is due to the fact that floating point numbers are represented by finite precision. A computer cannot store floating point numbers with perfect precision, instead the number is represented by a finite number of bytes. This type of error can not be reduced by reducing the number of calculations in the numerical algorithm. Truncation error occurs when we make a discrete approximation to a continuous function. It is also called discretization error, and is introduced at each step of the method. Using Euler's method (1.5) as an example, we can derive the local truncation error. If $y(t)$ is the solution of (1.1), the local truncation error, $TE(t, h)$, of Euler's method (1.5) is defined by

$$TE(t_n, h) = \frac{y(t_n + h) - y(t_n)}{h} - f(t_n, y(t_n)). \quad (1.11)$$

Using the Taylor's formula for remainder, we get

$$TE(t_n, h) = \frac{h}{2!} y''(c)$$

where $t_n < c < t_{n+1}$. The value of c exists only for theoretically and therefore the exact error can not be calculated. On the other hand, an upper bound on the absolute value of the error is $\frac{Mh}{2!}$ where $M = \max_{t_n < c < t_{n+1}} |y''|$. Although round-off error and local truncation error arise from different sources, these two types of errors are not independent of each other. For example, the truncation error can usually be reduced by using a smaller step size h , but this may yields greater rounding error because of the increase in the number of computation. Truncation error is the dominant factor in determining the accuracy of numerical solutions of IVPs and henceforth rounding error is ignored, in most situations [17].

The accuracy of a numerical method is said to be of order p if

$$TE(t_n, h) = O(h^p). \quad (1.12)$$

Euler's method (1.5) and implicit Euler method (1.8) are first-order accurate methods, while the trapezoidal rule (1.9) and the implicit midpoint rule (1.10) are second-order accurate methods.

A numerical method is said to be consistent approximation to the differential equation (1.1) if

$$TE(t_n, h) \rightarrow 0, \quad \text{as } h \rightarrow 0. \quad (1.13)$$

All methods described above are consistent methods.

1.2.1 Runge-Kutta Methods

One of the most important one-step method to approximate the solution of the IVP (1.1) is the Runge-Kutta method. Runge-Kutta methods do not require the computation of higher derivatives on the contrary of the Taylor's series method [17]. Runge-Kutta methods evaluates f several times between t_k and t_{k+1} .

A general s -stage Runge-Kutta method for the solution of the non-autonomous system of first-order ordinary differential equations

$$y'(t) = f(t, y(t)), \quad y(t_0) = y_0 \quad (1.14)$$

is given by

$$\begin{aligned} k_i &= f\left(t_n + c_i h, y_n + h \sum_{j=1}^s a_{ij} k_j\right), \quad i = 1, \dots, s \\ y_{n+1} &= y_n + h \sum_{i=1}^s b_i k_i \end{aligned} \quad (1.15)$$

where $b_i, a_{ij}, (i, j, \dots, s)$ are real number and we assume that the following holds:

$$c_i = \sum_{j=1}^s a_{ij}, \quad i = 1, \dots, s.$$

Here the full matrix (a_{ij}) is allowed to non-zero coefficients. The Runge-Kutta method (1.15) can be written as

$$\begin{aligned} k_1 &= f(t_n + c_1 h, y_n + h(a_{11}k_1 + \dots + a_{1s}k_s)) \\ k_2 &= f(t_n + c_2 h, y_n + h(a_{21}k_1 + \dots + a_{2s}k_s)) \\ k_3 &= f(t_n + c_3 h, y_n + h(a_{31}k_1 + \dots + a_{3s}k_s)) \\ &\vdots \\ k_s &= f(t_n + c_s h, y_n + h(a_{s1}k_1 + \dots + a_{ss}k_s)) \end{aligned}$$

and

$$y_{n+1} = y_n + h(b_1 k_1 + \dots + b_s k_s).$$

Runge-Kutta methods are often represented using the Butcher array

$$\begin{array}{c|ccc} c_1 & a_{11} & a_{12} & \cdots & a_{1s} \\ c_2 & a_{21} & a_{22} & \cdots & a_{2s} \\ \vdots & \vdots & \vdots & & \vdots \\ c_s & a_{s1} & a_{s2} & \cdots & a_{ss} \\ \hline & b_1 & b_2 & \cdots & b_s \end{array} = \quad (1.16)$$

The Runge-Kutta method (1.15) is said to be explicit if

$$a_{ij} = 0, \quad \text{for all } 1 \leq i \leq j \leq s$$

and implicit otherwise. It is called diagonally-implicit Runge-Kutta method if $a_{ij} = 0$ for $i < j$ and at least one $a_{ii} \neq 0$. Runge Kutta method (1.15) is said to be consistent [16] with the equation (1.14) if and only if

$$\sum_{i=1}^s b_i = 1.$$

1.3 Adjoint method and Composition method

We first present the composition method for ordinary differential equations (ODEs).

We know that every one-step integrator for $y' = f(y)$ can be

$$y_{n+1} = \phi_h(y_n) \quad (1.17)$$

where ϕ_h is the operator corresponding to the integrator, and h is the step-length. Sometimes one has a method ϕ_h (the basic method) with good geometric properties and the idea is to construct a new method of the form

$$\psi_h = \phi_{\gamma_s h} \circ \phi_{\gamma_{s-1} h} \circ \cdots \circ \phi_{\gamma_1 h} \quad (1.18)$$

where $\gamma_1, \dots, \gamma_s$ are real numbers chosen in such a way that ψ_h is of higher order than ϕ_h . In this way one increases the order of accuracy while preserving the desirable properties the basic method $\phi(h)$ has, as long as the geometric property is preserved by composition. This is true, in particular, if ϕ is symplectic [44] or volume preserving [6].

If a numerical one-step method ϕ_h is called symmetric or time-reversible [6] if it satisfies

$$\phi_h \circ \phi_{-h} = id \quad (1.19)$$

That is a method (1.17) is symmetric if it remains unchanged when if $y_n \leftrightarrow y_{n+1}$ and $h \leftrightarrow -h$ are swapped. For example, the implicit midpoint rule symmetric since if $y_n \leftrightarrow y_{n+1}$ and $h \leftrightarrow -h$ are swapped in (1.10), we get

$$y_n = y_{n+1} - hf\left(\frac{y_{n+1} + y_n}{2}\right)$$

which yields the method (1.10). Similarly, one can show that the trapezoidal rule (1.9) is symmetric, too.

The adjoint method ϕ^* corresponding to (1.17) is the method

$$y_{n+1} = \phi_h^*(y_n) \quad (1.20)$$

is the inverse map of the original method with reversible time step $-h$ defined by the relation

$$y_n = \phi_{-h}^*(y_{n+1}).$$

In other words, $\phi_h^* = \phi_{-h}^{-1}$. For example, the adjoint of the explicit Euler method (1.5) is the implicit Euler method (1.8). If the method is symmetric then $\phi_h^* = \phi_h$. For any two one-step methods ϕ_h and ψ_h , the adjoint method satisfies the properties $(\phi_h^*)^* = \phi_h$ and $(\phi_h \circ \psi_h)^* = \psi_h^* \circ \phi_h^*$.

Theorem 1.3.1 [6] *Let ϕ_h is a one-step method of order p . If*

$$\begin{aligned}\gamma_1 + \cdots + \gamma_s &= 1 \\ \gamma_1^{p+1} + \cdots + \gamma_s^{p+1} &= 0\end{aligned}\tag{1.21}$$

then the composition method (1.18) has at least of order $p + 1$.

The equations (1.21) have no real solutions for odd p . Therefore the order is increased only for p even. If the composition (1.18) is replaced by the more general formula

$$\psi_h = \phi_{\alpha_s h} \circ \phi_{\beta_s h}^* \circ \cdots \circ \phi_{\alpha_1 h} \circ \phi_{\beta_1 h}^*\tag{1.22}$$

the order condition for order $p + 1$ analogous to (1.21) becomes

$$\begin{aligned}\alpha_1 + \beta_1 \cdots + \alpha_s + \beta_s &= 1 \\ \alpha_1^{p+1} + (-1)^p \beta_1^{p+1} + \cdots + \alpha_s^{p+1} + (-1)^p \beta_s^{p+1} &= 0.\end{aligned}\tag{1.23}$$

This equations have a solution for odd and even p , in contrary to the system (1.21). In particular, if the method ϕ is first-order, i.e. $p = 1$ and $s = 1$, the solution is $\alpha_1 = \beta_1 = 1/2$, which turns every first-order one-step method into a second-order symmetric method

$$\psi_h = \phi_{h/2} \circ \phi_{h/2}^*.\tag{1.24}$$

The thesis is organized as follows: In Chapter 2, Hamiltonian ODEs are introduced and some examples are given. The Average Vector Field (AVF), the partitioned Average Vector Field (PAVF) methods for Hamiltonian systems are given. In conjunction with the adjoint PAVF method, the PAVF composition (PAVF-C) and the PAVF plus (PAVF-P) methods are also discussed. Chapter 3 is devoted to the numerical solution of Hamiltonian PDEs by using the AVF, PAVF, PAVF-C and the PAVF-P methods. In this thesis, this is the first time that energy persevering AVF, PAVF, PAVF-C and PAVF-P methods are derived for the numerical solution of the Zakharov system. Some conclusions based on our findings and numerical results for the Zakharov system are also drawn in this chapter. At last, we give some the conclusion remarks in Chapter 4.

CHAPTER 2

HAMILTONIAN ORDINARY DIFFERENTIAL EQUATIONS

For general Hamiltonian system, conservation of Hamiltonian (i.e. the energy) cannot be guaranteed in general. To get rid of this problem, many studies have been done for numerical methods that directly preserve the energy of the Hamiltonian system. In order to get an idea about the history of geometric integration, one can refer to the monograph [6]. Recently, a new class of energy-preserving methods called averaged vector field (AVF) method was introduced in [49]. It is a one-step method which requires only function evaluation of the vector field. The AVF method is a B-series scheme of the second order. As a discrete gradient method, it preserves exactly the energy integral for any canonical Hamiltonian system. The AVF method is first written down in [50] as a specific discrete gradient method by taking a mean-value discrete gradient as the discrete counterpart of the gradient operator. In [21] two energy-preserving high-order average vector field (AVF) compact finite difference techniques for solving variable coefficient nonlinear wave equations with periodic boundary conditions were developed and analyzed. In [41] two locally exact and energy-preserving modifications of the AVF method, namely AVF-LEX (of the third order) and AVF-SLEX (of the fourth order) are proposed. Applications to spherically symmetric potentials are given, including a compact explicit expression for the AVF scheme for the Coulomb-Kepler problem. In [42] the energy preserving AVF integrator is applied to one and two dimensional Schrödinger equations using the symmetric split-step technique. In [43] the AVF method is used for multisymplectic formulations of Hamiltonian PDEs in order to create algorithms that preserve both energy and momentum. In [51] a high order energy preserving scheme for the strongly coupled nonlinear Schrödinger system is proposed by using the AVF method.

2.1 Hamiltonian Systems

We start by presenting some notation. Let Ω be a domain in \mathbb{R}^{2d} of the points $(p, q) = (p_1, \dots, p_d, q_1, \dots, q_d)$. Let I be an open interval of the real line \mathbb{R} of the variable t .

Definition 2.1.1 *If $H = H(p, q, t)$ is a sufficiently smooth real function in the product $\Omega \times I$, then the dynamical system*

$$\begin{aligned} \frac{dq_i}{dt} &= \frac{\partial H}{\partial p_i}, \\ \frac{dp_i}{dt} &= -\frac{\partial H}{\partial q_i}, \quad i = 1, \dots, d \end{aligned} \quad (2.1)$$

is called a Hamiltonian system and H is the Hamiltonian function (or the energy) of the system.

The number of degrees of freedom of a Hamiltonian system is the number of the pairs (p_i, q_i) in the Hamiltonian system (2.1), i.e. the number d is the number of degrees of freedom of the system. The phase-space Ω is therefore even dimensional. We set $z = (p_i, q_i)^T$ and consider the Hamiltonian system (2.1) of the form

$$\frac{dy}{dt} = f(y) = J\nabla H(y) \quad (2.2)$$

where $y \in \mathbb{R}^m$, $m = 2d$, and

$$J = \begin{pmatrix} 0 & I_{d \times d} \\ -I_{d \times d} & 0 \end{pmatrix}$$

is a $m \times m$ skew-symmetric matrix, and $H(y)$ is a sufficiently differentiable Hamiltonian, or the energy. The most fundamental property of the Hamiltonian system is the conservation of the Hamiltonian. If the Hamiltonian is autonomous, i.e. $H = H(p, q)$

$$\frac{dH(y)}{dt} = (\nabla H(y))^T \frac{dy}{dt} = (\nabla H(y))^T J \nabla H(y) = 0. \quad (2.3)$$

The one-dimensional harmonic oscillator is an example for a Hamiltonian system (2.2). The equation of motion of the one-dimensional harmonic oscillator is

$$m \frac{d^2}{dt^2} x(t) = -kx(t), \quad x(t) \in \mathbb{R} \quad (2.4)$$

The system (2.4) describes the one-dimensional motion of a particle of mass m attached to an elastic helical spring with stiffness constant k (see Fig.2.1). Introducing

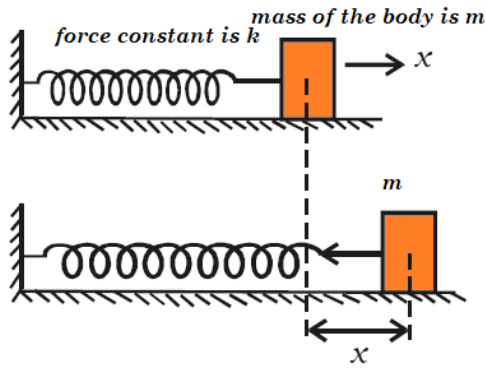


Figure 2.1: A simple harmonic oscillator in classical mechanics is a particle which is acted upon by a restoring force proportional to its displacement from its equilibrium position.

the position coordinate $q(t) = x(t)$ and the linear momentum $p(t) = mx'$ the equation (2.4) can be written as Hamiltonian system of equations

$$\begin{aligned} \frac{dq}{dt} &= \frac{p}{m} \\ \frac{dp}{dt} &= -kq \end{aligned} \quad (2.5)$$

where the Hamiltonian $H(q, p) = \frac{1}{2m}p^2 + \frac{k}{2}q^2$ represents the total energy of the system. If the Hamiltonian is separable, i.e

$$H(p, q) = T(p) + U(q)$$

then the equation (2.1) can be reduced to two simpler equations

$$\frac{dq}{dt} = \nabla T(p), \quad \frac{dp}{dt} = -\nabla U(q). \quad (2.6)$$

When problem (2.1) is of the form

$$H(p, q) = \frac{1}{2}p^T p - U(q)$$

then (2.1) reduces to a special second order equation

$$\frac{dq^2}{dt^2} = \nabla U(q).$$

Consider the autonomous differential equations

$$\frac{dy}{dt} = f(y) \quad (2.7)$$

where $y(t)$ is a vector or possibly a matrix. A non-constant function $I(y)$ is called a first integral of (2.7) if

$$I'(y)f(y) = 0$$

for all y . This implies that every solution $y(t)$ of (2.71.1) satisfies $I(y(t)) = I(y_0) = \text{Const.}$ Synonymously with first integral, the terms invariant or conserved quantity or constant of motion are also used. For instance, $I(u, v) = \ln u - u + 2 \ln v - v$ is the first-integral of the Lotka-Volterra system

$$\frac{du}{dt} = u(v - 2), \quad \frac{dv}{dt} = v(1 - u) \quad (2.8)$$

since

$$\begin{aligned} \frac{dI}{dt} &= \frac{d}{dt} (\ln u - u + 2 \ln v - v) \\ &= \frac{1}{u}u' - u' + \frac{2}{v}v' - v' \\ &= \frac{1}{u}(u(v - 2)) - (u(v - 2)) + \frac{2}{v}(v(1 - u)) - (v(1 - u)) \\ &= 0 \end{aligned}$$

Quadratic invariants are frequently encountered in applications. A quadratic function can be represented by $Q(y) = y^T C y$ where C is a square symmetric matrix. For any y , $Q(y)$ is an invariant of (2.7) if $y^T C f(y) = 0$, since

$$\begin{aligned} \frac{dQ}{dt}(y) &= (y')^T C y + y^T C y' = (f(y))^T C y + y^T C f(y) \\ &= (y^T C f(y))^T + y^T C f(y) = 0 \end{aligned}$$

because C is symmetric. An s -stage Runge-Kutta method conserves quadratic invariants if the coefficients of the method satisfy

$$b_i a_{ij} + b_j a_{ji} = b_i b_j, \quad i, j = 1, \dots, s. \quad (2.9)$$

Next, we consider differential equations of the form

$$\frac{dy}{dt} = A(y)y \quad (2.10)$$

where y is a vector. If $A(y)$ is skew-symmetric for all y , then the quadratic function $I(y) = y^T y$ is an invariant of (2.10). The Euler's equation has this property. The Euler equations describe the motion of a free rigid body, whose centre of mass is at the

origin, given by

$$\begin{aligned} y_1' &= a_1 y_2 y_3, & a_1 &= (I_2 - I_3)/I_2 I_3 \\ y_2' &= a_2 y_3 y_1, & a_2 &= (I_3 - I_1)/I_3 I_1 \\ y_3' &= a_3 y_1 y_2, & a_3 &= (I_1 - I_2)/I_1 I_2 \end{aligned} \quad (2.11)$$

where the angular momentum in the body frame is represented by the vector $y = (y_1, y_2, y_3)^T$, and the primary moments of inertia are I_1, I_2, I_3 [6]. It can be written in the form of (2.10) as follows:

$$\begin{pmatrix} y_1' \\ y_2' \\ y_3' \end{pmatrix} = \begin{pmatrix} 0 & y_3/I_3 & -y_2/I_2 \\ -y_3/I_3 & 0 & y_1/I_1 \\ y_2/I_2 & -y_1/I_1 & 0 \end{pmatrix} \begin{pmatrix} y_1 \\ y_2 \\ y_3 \end{pmatrix}$$

It is easy to show that $y_1 y_1' + y_2 y_2' + y_3 y_3' = 0$, hence $I(y) = y_1^2 + y_2^2 + y_3^2$ is a quadratic invariant of the system. It's worth noting that the system is a Hamiltonian system with Hamiltonian $H(y_1, y_2, y_3) = \frac{1}{2}(\frac{y_1^2}{I_1} + \frac{y_2^2}{I_2} + \frac{y_3^2}{I_3})$ which is the second quadratic invariant.

2.2 The Average Vector Field Method

One of the most important characteristics of a Hamiltonian wave equation is the conservation of the energy function. Discrete gradient (DG) approaches are of the most popular ways for creating energy preserving schemes for ordinary differential equations [10]. This was first investigated in [45] by Gonzales. Then a discrete variational approach for solving the nonlinear wave equation was proposed [46]. Hamiltonian boundary value approaches were developed by Brugnano et al. [47], Iavernaro and Trigiante [48]. If V is a differentiable function on R , then a discrete gradient is a vector-valued function $\bar{\nabla}V = \bar{\nabla}V(y, y')$ which satisfied

$$\begin{aligned} \bar{\nabla}V(y, y')^T (y - y') &= V(y) - V(y') \\ \bar{\nabla}V(y, y) &= \nabla V(y). \end{aligned} \quad (2.12)$$

Several types of DG methods have been found in the literature [18]. Itoh and Abe [19] have been constructed families of discrete gradients in terms of difference equations. One example in R^2 is

$$\bar{\nabla}V(y, y') = \begin{pmatrix} \frac{V(x, y) - V(x', y)}{x - x'} \\ \frac{V(x', y) - V(x', y')}{y - y'} \end{pmatrix}. \quad (2.13)$$

Another discrete gradient has been constructed in [20] as the average value of gradient. Suppose (y_1, \dots, y_d) are the coordinates of the domain $\Omega \subset R^d$, and V a scalar function on Ω with gradient

$$\nabla V = \left(\frac{\partial V_1}{\partial x_1}, \dots, \frac{\partial V_d}{\partial x_d} \right). \quad (2.14)$$

Consider the straight line path from \mathbf{y} to \mathbf{y}' in the domain Ω . Then, the discrete gradient \bar{V} is defined as

$$\bar{\nabla} V(\mathbf{y}, \mathbf{y}') := (\bar{V}_1, \dots, \bar{V}_d), \quad \bar{V}_i := \int_0^1 V_i(\xi \mathbf{y}' + (1 - \xi) \mathbf{y}) d\xi. \quad (2.15)$$

The vector-valued function $\bar{\nabla} V$ in (2.15) is discrete gradient, since

$$\begin{aligned} \sum_{i=1}^d (\bar{\nabla} V)_i(\mathbf{y} - \mathbf{y}') &= \int_0^1 \sum_{i=1}^d V_i(\xi \mathbf{y}' + (1 - \xi) \mathbf{y})(\mathbf{y} - \mathbf{y}') d\xi. \\ &= \int_0^1 \sum_{i=1}^d \frac{d}{dt} V(\xi \mathbf{y}' + (1 - \xi) \mathbf{y}) d\xi. \\ &= V(\mathbf{y}') - V(\mathbf{y}) \end{aligned} \quad (2.16)$$

and

$$\lim_{\mathbf{y} \rightarrow \mathbf{y}'} \bar{\nabla} V(\mathbf{y}, \mathbf{y}') = \nabla V(\mathbf{y}'). \quad (2.17)$$

The conservation of the energy function is one of the most relevant features characterizing a Hamiltonian system. Methods that exactly preserve energy have been considered for several decades and many energy-preserving methods have been proposed [14, 15]. A new class of energy-preserving method called Average Vector Field (AVF) method was introduced [4]. For ordinary differential equation

$$\frac{dy}{dt} = f(y) \quad (2.18)$$

the second-order AVF method is defined by [3, 4]

$$\frac{y^{n+1} - y^n}{\tau} = \int_0^1 f(\xi y^{n+1} + (1 - \xi) y^n) d\xi. \quad (2.19)$$

where τ denotes the times step. The AVF method (2.19) applied to the Hamiltonian system (2.2) can be written as

$$\frac{y^{n+1} - y^n}{\tau} = J \int_0^1 \nabla H(\xi y^{n+1} + (1 - \xi) y^n) d\xi \quad (2.20)$$

Theorem 2.2.1 *The AVF method (2.20) preserves the Hamiltonian $H(y)$ of the system (2.2) exactly, and satisfies*

$$H(y^{n+1}) = H(y^n). \quad (2.21)$$

Proof.

$$\begin{aligned}
\frac{1}{\tau} (H(y^{n+1}) - H(y^n)) &= \frac{1}{\tau} \int_0^1 \frac{d}{d\xi} H(\xi y^{n+1} + (1-\xi)y^n) d\xi \\
&= \left(\int_0^1 \nabla H(\xi y^{n+1} + (1-\xi)y^n) d\xi \right)^T \left(\frac{y^{n+1} - y^n}{\tau} \right) \\
&= \left(\int_0^1 \nabla H(\xi y^{n+1} + (1-\xi)y^n) d\xi \right)^T J \\
&\quad \times \left(\int_0^1 \nabla H(\xi y^{n+1} + (1-\xi)y^n) d\xi \right) \\
&= 0
\end{aligned} \tag{2.22}$$

It follows that the Hamiltonian H is preserved at every time step. \square

A higher order energy preserving AVF method method [4, 5] is

$$\frac{z^{n+1} - z^n}{\tau} = (\delta_j^i + \alpha h^2 f_k^i(\hat{z}) f_j^k(\hat{z})) \int_0^1 f^j(\xi z^{n+1} + (1-\xi)z^n) d\xi. \tag{2.23}$$

where α is an arbitrary constant, δ_j^i is the Kronecker delta, and we can take e.g. $\hat{z} = z_n$ or $\hat{z} = \frac{z_n + z_{n+1}}{2}$. For $\alpha = 0$, we recover the second order method (2.19). For $\alpha = -1/12$ and $\hat{z} = z_n$, the method is of order three. For $\alpha = -1/12$ and $\hat{z} = \frac{z_n + z_{n+1}}{2}$ the method is of order four. A new six order AVF method is obtained in [5].

2.3 The Partitioned Average Vector Field Method

Recently, a more efficient AVF based method namely the partitioned Average Vector Field (PAVF) method was introduced in [1]. In this subsection, we will review some material from [1]. The partitioned AVF (PAVF) method for the Hamiltonian system (2.2) is defined by [1]

$$\frac{1}{\tau} \begin{pmatrix} p^{n+1} - p^n \\ q^{n+1} - q^n \end{pmatrix} = J \begin{pmatrix} \int_0^1 H_p(\xi p^{n+1} + (1-\xi)p^n, q^n) d\xi \\ \int_0^1 H_p(p^{n+1}, \xi q^{n+1} + (1-\xi)q^n) d\xi \end{pmatrix} \tag{2.24}$$

Like the AVF method (2.20), the PAVF method (2.24) preserves the Hamiltonian $H(p, q)$ of the system (2.2), exactly, and stisfies (2.21), too. In order to prove this fact, take the scalar product with

$$\left(\int_0^1 H_p(\xi p^{n+1} + (1-\xi)p^n, q^n)^T d\xi, \int_0^1 H_p(p^{n+1}, \xi q^{n+1} + (1-\xi)q^n)^T d\xi \right)^T$$

on both sides of (2.24) and get

$$\begin{aligned}
0 &= \frac{1}{\tau} \int_0^1 H_p(\xi p^{n+1} + (1-\xi)p^n, q^n)^T d\xi(p^{n+1} - p^n) \\
&\quad + \frac{1}{\tau} \int_0^1 H_p(p^{n+1}, \xi q^{n+1} + (1-\xi)q^n)^T d\xi(q^{n+1} - q^n) \\
&= \frac{1}{\tau} \int_0^1 \frac{d}{d\xi} \left(H(\xi p^{n+1} + (1-\xi)p^n, q^n) + H(p^{n+1}, \xi q^{n+1} + (1-\xi)q^n) \right) d\xi \\
&= \frac{1}{\tau} \left(H(p^{n+1}, q^n) - H(p^n, q^n) + H(p^{n+1}, q^{n+1}) - H(p^{n+1}, q^n) \right) \\
&= \frac{1}{\tau} \left(H(p^n, q^n) - H(p^{n+1}, q^{n+1}) \right)
\end{aligned}$$

which is (2.21). The PAVF method (2.24) is a one-step first-order method. For separable Hamiltonian $H(p, q) = T(p) + V(q)$, AVF method (2.20) and PAVF method (2.24) are equivalent. For non-constant skew-symmetric matrix $J = J(p, q)$, the PAVF-like method (2.24) can be written as

$$\frac{1}{\tau} \begin{pmatrix} p^{n+1} - p^n \\ q^{n+1} - q^n \end{pmatrix} = J(p^n, q^n) \begin{pmatrix} \int_0^1 H_p(\xi p^{n+1} + (1-\xi)p^n, q^n) d\xi \\ \int_0^1 H_p(p^{n+1}, \xi q^{n+1} + (1-\xi)q^n) d\xi \end{pmatrix} \quad (2.25)$$

which preserves the Hamiltonian, i.e. (2.25) satisfies (2.21), too. In order to improve the efficiency in the method (2.25), one can choose a better approximation to $J(p, q)$.

If the PAVF method (2.24) is denoted by Φ_τ , then reversing the path order in Φ_τ , the method Φ_τ^* which is adjoint to Φ_τ can be given as

$$\frac{1}{\tau} \begin{pmatrix} p^{n+1} - p^n \\ q^{n+1} - q^n \end{pmatrix} = J \begin{pmatrix} \int_0^1 H_p(\xi p^{n+1} + (1-\xi)p^n, q^{n+1}) d\xi \\ \int_0^1 H_p(p^n, \xi q^{n+1} + (1-\xi)q^n) d\xi \end{pmatrix}. \quad (2.26)$$

The PAVF composition (PAVF-C) method is defined by coupling with the adjoint PAVF method

$$\Psi_\tau = \Phi_{\frac{\tau}{2}}^* \circ \Phi_{\frac{\tau}{2}}, \quad (2.27)$$

and partitioned AVF plus (PAVF-P) method is defined as

$$\hat{\Psi}_\tau := \frac{1}{2}(\Phi_\tau^* + \Phi_\tau), \quad (2.28)$$

respectively. Methods (2.27) and (2.28) are both second order and preserves the energy of the Hamiltonian (2.2).

Now we consider a more general for the Hamiltonian system (2.2)

$$\frac{d}{dt} \begin{pmatrix} \hat{z}_1 \\ \hat{z}_2 \\ \vdots \\ \hat{z}_{m-1} \\ \hat{z}_m \end{pmatrix} = J \begin{pmatrix} H_{\hat{z}_1}(\hat{z}_1, \hat{z}_2, \dots, \hat{z}_{m-1}, \hat{z}_m) \\ H_{\hat{z}_2}(\hat{z}_1, \hat{z}_2, \dots, \hat{z}_{m-1}, \hat{z}_m) \\ \vdots \\ H_{\hat{z}_{m-1}}(\hat{z}_1, \hat{z}_2, \dots, \hat{z}_{m-1}, \hat{z}_m) \\ H_{\hat{z}_m}(\hat{z}_1, \hat{z}_2, \dots, \hat{z}_{m-1}, \hat{z}_m) \end{pmatrix} \quad (2.29)$$

where $z = (\hat{z}_1, \hat{z}_2, \dots, \hat{z}_{m-1}, \hat{z}_m)$ where $\hat{z}_k \in R^d, k = 1, 2, \dots, \bar{m}$ with $m = \bar{m}d$ even, and J is a $m \times m$ skew-symmetric matrix. For the system (2.29), the PAVF method can be defined by

$$\frac{1}{\tau} \begin{pmatrix} \hat{z}_1^{n+1} - \hat{z}_1^n \\ \hat{z}_2^{n+1} - \hat{z}_2^n \\ \vdots \\ \hat{z}_{\bar{m}-1}^{n+1} - \hat{z}_{\bar{m}-1}^n \\ \hat{z}_{\bar{m}}^{n+1} - \hat{z}_{\bar{m}}^n \end{pmatrix} = J \begin{pmatrix} \int_0^1 H_{\hat{z}_1}(\xi \hat{z}_1^{n+1} + (1-\xi)\hat{z}_1^n, \hat{z}_2^n, \dots, \hat{z}_{\bar{m}-1}^n, \hat{z}_{\bar{m}}^n) d\xi \\ \int_0^1 H_{\hat{z}_2}(\hat{z}_1^{n+1}, \xi \hat{z}_2^{n+1} + (1-\xi)\hat{z}_2^n, \dots, \hat{z}_{\bar{m}-1}^n, \hat{z}_{\bar{m}}^n) d\xi \\ \vdots \\ \int_0^1 H_{\hat{z}_{\bar{m}-1}}(\hat{z}_1^{n+1}, \hat{z}_2^{n+1}, \dots, \xi \hat{z}_{\bar{m}-1}^{n+1} + (1-\xi)\hat{z}_{\bar{m}-1}^n, \hat{z}_{\bar{m}}^n) d\xi \\ \int_0^1 H_{\hat{z}_{\bar{m}}}(\hat{z}_1^{n+1}, \hat{z}_2^{n+1}, \dots, \hat{z}_{\bar{m}-1}^{n+1}, \xi \hat{z}_{\bar{m}}^{n+1} + (1-\xi)\hat{z}_{\bar{m}}^n) d\xi \end{pmatrix} \quad (2.30)$$

and its adjoint scheme can be defined by

$$\frac{1}{\tau} \begin{pmatrix} \hat{z}_1^{n+1} - \hat{z}_1^n \\ \hat{z}_2^{n+1} - \hat{z}_2^n \\ \vdots \\ \hat{z}_{\bar{m}-1}^{n+1} - \hat{z}_{\bar{m}-1}^n \\ \hat{z}_{\bar{m}}^{n+1} - \hat{z}_{\bar{m}}^n \end{pmatrix} = S_{\bar{m}d} \begin{pmatrix} \int_0^1 H_{\hat{z}_1}(\xi \hat{z}_1^{n+1} + (1-\xi)\hat{z}_1^n, \hat{z}_2^{n+1}, \dots, \hat{z}_{\bar{m}-1}^{n+1}, \hat{z}_{\bar{m}}^{n+1}) d\xi \\ \int_0^1 H_{\hat{z}_2}(\hat{z}_1^n, \xi \hat{z}_2^{n+1} + (1-\xi)\hat{z}_2^n, \dots, \hat{z}_{\bar{m}-1}^{n+1}, \hat{z}_{\bar{m}}^{n+1}) d\xi \\ \vdots \\ \int_0^1 H_{\hat{z}_{\bar{m}-1}}(\hat{z}_1^n, \hat{z}_2^n, \dots, \xi \hat{z}_{\bar{m}-1}^{n+1} + (1-\xi)\hat{z}_{\bar{m}-1}^n, \hat{z}_{\bar{m}}^{n+1}) d\xi \\ \int_0^1 H_{\hat{z}_{\bar{m}}}(\hat{z}_1^n, \hat{z}_2^n, \dots, \hat{z}_{\bar{m}-1}^n, \xi \hat{z}_{\bar{m}}^{n+1} + (1-\xi)\hat{z}_{\bar{m}}^n) d\xi \end{pmatrix}. \quad (2.31)$$

The PAVF-C and the PAVF-P method can be defined analogously. Following the proof of the theorem (2.2.1), it can be shown that the PAVF method (2.30) preserves the Hamiltonian $H(z)$ of the general system (2.29) exactly, and satisfies (2.21).

2.4 Numerical example

In this section, we reproduced AVF, PAVF, PAVF-C and PAVF-P methods for the Henon-Heiles system from [1].

2.4.1 Hénon-Heiles System

We consider the Henon-Heiles system

$$z' = J\nabla H(z), \quad (2.32)$$

where

$$H(z) = \frac{1}{2}(q_1^2 + q_2^2 + p_1^2 + p_2^2) + q_1^2 q_2 - \frac{1}{3} q_2^3, \quad (2.33)$$

$z = (q_1, q_2, p_1, p_2)^T$ and

$$J = \begin{pmatrix} 0 & I \\ -I & 0 \end{pmatrix}$$

with I a 2×2 identity matrix.

Let $t_n = t_0 + nh$, $n = 0, 1, 2, \dots, N$ be the regular grids of the integral domain $[t_0, T]$, z^n be an approximation to $z(t_n)$, and h be the space step. The second order AVF method (2.20) applied to Eq. (2.32) is

$$\begin{aligned} \frac{1}{\tau}(q_1^{n+1} - q_1^n) &= \frac{1}{2}(p_1^{n+1} + p_1^n) \\ \frac{1}{\tau}(q_2^{n+1} - q_2^n) &= \frac{1}{2}(p_2^{n+1} + p_2^n), \\ \frac{1}{\tau}(p_1^{n+1} - p_1^n) &= -\left(\frac{1}{2}(q_1^{n+1} + q_1^n) + \frac{1}{3}(q_1^{n+1} q_2^{n+1} + 4q_1^{n+\frac{1}{2}} q_2^{n+\frac{1}{2}} + q_1^n q_2^n)\right), \\ \frac{1}{\tau}(p_2^{n+1} - p_2^n) &= \frac{1}{3}((q_2^{n+1})^2 + q_2^{n+1} q_2^n + (q_2^n)^2 - (q_1^{n+1})^2 - q_1^{n+1} q_1^n - (q_1^n)^2) \\ &\quad - \frac{1}{2}(q_2^{n+1} + q_2^n). \end{aligned} \quad (2.34)$$

The first order PAVF method (2.24) applied to Eq. (2.32) is

$$\frac{1}{\tau} \begin{pmatrix} q_1^{n+1} - q_1^n \\ q_2^{n+1} - q_2^n \\ p_1^{n+1} - p_1^n \\ p_2^{n+1} - p_2^n \end{pmatrix} = J \begin{pmatrix} \int_0^1 H_{q_1}(\xi q_1^{n+1} + (1-\xi)q_1^n, q_2^n, p_1^n, p_2^n) d\xi \\ \int_0^1 H_{q_2}(q_1^{n+1}, \xi q_2^{n+1} + (1-\xi)q_2^n, p_1^n, p_2^n) d\xi \\ \int_0^1 H_{p_1}(q_1^{n+1}, q_2^{n+1}, \xi p_1^{n+1} + (1-\xi)p_1^n, p_2^n) d\xi \\ \int_0^1 H_{p_2}(q_1^{n+1}, q_2^{n+1}, p_1^{n+1}, \xi p_2^{n+1} + (1-\xi)p_2^n) d\xi \end{pmatrix} \quad (2.35)$$

Equations (2.35) can be written as

$$\begin{aligned} \frac{1}{\tau}(q_1^{n+1} - q_1^n) &= \frac{1}{2}(p_1^{n+1} + p_1^n), \\ \frac{1}{\tau}(q_2^{n+1} - q_2^n) &= \frac{1}{2}(p_2^{n+1} + p_2^n), \\ \frac{1}{\tau}(p_1^{n+1} - p_1^n) &= -\left(\frac{1}{2}(q_1^{n+1} + q_1^n) + (q_1^{n+1} + q_1^n)q_2^n\right), \\ \frac{1}{\tau}(p_2^{n+1} - p_2^n) &= -\left(\frac{1}{2}(q_2^{n+1} + q_2^n) + (q_1^{n+1})^2\right) + \frac{1}{3}((q_2^{n+1})^2 + q_2^{n+1} q_2^n + (q_2^n)^2). \end{aligned} \quad (2.36)$$

The PAVF method (2.35) is semi-implicit that is values q_1^{n+1} and p_1^{n+1} can be determined from the first and the third equation explicitly in (2.35), and only q_2^{n+1} , p_2^{n+1} are determined by iteration. On the other hand, the AVF method (2.34) is fully-implicit which requires more computational time than the PAVF method (2.35). Therefore, we can say that the PAVF method (2.35) is simpler and effective than the AVF method (2.34).

The adjoint method corresponding to the PAVF method (2.35) can be written analogously. Using the PAVF method (2.35) together with its adjoint method, the second-order energy preserving PAVF-C method for the Henon-Heiles system (2.32) can be derived as

$$\begin{aligned}
\frac{2}{\tau}(q_1^* - q_1^n) &= \frac{1}{2}(p_1^* + p_1^n), \\
\frac{2}{\tau}(q_2^* - q_2^n) &= \frac{1}{2}(p_2^* + p_2^n), \\
\frac{2}{\tau}(p_1^* - p_1^n) &= -\left(\frac{1}{2}(q_1^* + q_1^n) + (q_1^* + q_1^n)q_2^n\right) \\
\frac{2}{\tau}(p_2^* - p_2^n) &= -\left(\frac{1}{2}(q_2^* + q_2^n) + (q_1^*)^2\right) + \frac{1}{3}((q_2^*)^2 + q_2^*q_2^n + (q_2^n)^2) \\
\frac{2}{\tau}(q_1^{n+1} - q_1^*) &= \frac{1}{2}(p_1^{n+1} + p_1^*), \\
\frac{2}{\tau}(q_2^{n+1} - q_2^*) &= \frac{1}{2}(p_2^{n+1} + p_2^*), \\
\frac{2}{\tau}(p_1^{n+1} - p_1^*) &= -\left(\frac{1}{2}(q_1^{n+1} - q_1^*) + (q_1^{n+1} - q_1^*)q_2^{n+1}\right), \\
\frac{2}{\tau}(p_2^{n+1} - p_2^*) &= -\left(\frac{1}{2}(q_2^{n+1} - q_2^*) + (q_1^*)^2\right) + \frac{1}{3}((q_2^{n+1})^2 + q_2^{n+1}q_2^* + (q_2^*)^2).
\end{aligned} \tag{2.37}$$

and the corresponding second-order energy preserving PAVF-P method can be written as

$$\begin{aligned}
\frac{1}{\tau}(q_1^{n+1} - q_1^n) &= \frac{1}{2}(p_1^{n+1} + p_1^n), \\
\frac{1}{\tau}(q_2^{n+1} - q_2^n) &= \frac{1}{2}(p_2^{n+1} + p_2^n), \\
\frac{1}{\tau}(p_1^{n+1} - p_1^n) &= -\frac{1}{2}(q_1^{n+1} + q_1^n + (q_1^{n+1} + q_1^n)(q_2^{n+1} + q_2^n)) \\
\frac{1}{\tau}(p_2^{n+1} - p_2^n) &= -\frac{1}{2}(q_2^{n+1} + q_2^n + (q_1^{n+1})^2 + (q_1^n)^2) \\
&\quad + \frac{1}{3}((q_2^{n+1})^2 + q_2^{n+1}q_2^n + (q_2^n)^2).
\end{aligned} \tag{2.38}$$

It is worth noting that the semi-implicit nature of the PAVF method is reflected into the PAVF-C method. In contrast, this is no longer satisfied by the PAVF-P method in view of the third equation in (2.38). The Henon-Heiles system (2.32) is one of the most simple, classical and characteristic Hamiltonian systems. It has a finite energy of escape H_{esc} which is equal to 1/6 [11]. For values of energy $H < H_{esc}$, the trajectories of the system are closed thus making escape impossible. However, for larger energy levels $H > H_{esc}$, the trajectories open and three exit channels appear through which

the test particles may escape to infinity. In order to test the performance of the AVF method (2.35), PAVF method (2.36), PAVF-C method (2.37) and the PAVF-P method (2.38), we explore the orbital structure of the Henon-Heiles system (2.32). We choose $H^0 = 1/6$ and $H^0 = 0.02$ with initial conditions (q_1^0, q_2^0, p_2^0) and see if there is an escape in trajectories. The leaving initial condition p_1^0 will be found from (2.33). Accuracy of the methods will be measured by using the relative error in energy defined by

$$err(H^n) = \frac{|H^n - H^0|}{|H^0|}, \quad (2.39)$$

where H^n is value of the Hamiltonian H in (2.33) at $t = t_n$.

Figure 2.2 represents the numerical trajectory with the initial condition $(q_1^0, q_2^0, p_2^0) = (0.1, -0.5, 0)$ for time step $\tau = 0.2$. From the figure, we can see that trajectories of all energy preserving methods stay within a triangle. The numerical trajectories never escape the triangle for any values of t and represents the chaotic orbit. Figure 2.3 represents the corresponding relative energy errors for all methods. The Fig. 2.3 verifies that the energy is preserved by all methods within the machine accuracy. The box orbits corresponding to the energy $H = 0.02$ for all energy preserving methods are represented in Fig.2.4. The initial conditions are $(q_1^0, q_2^0, p_2^0) = (0.1, -0.082, 0)$. Again, we see that curves of the system are close and trajectories do not escape to infinity. We presents the corresponding relative energy errors in Fig. 2.5. We see that PAVF, PAVF-C and PAVF-P methods preserves the energy better than the AVF method.

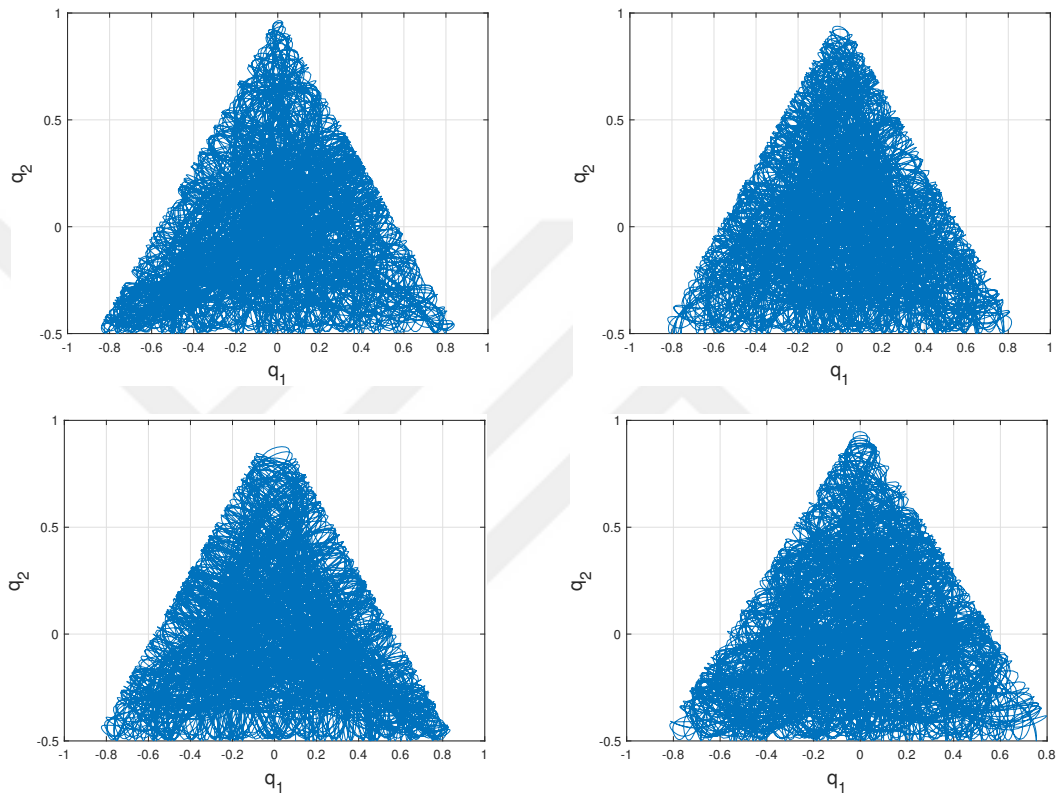


Figure 2.2: Chaotic orbit of the four energy preserving methods for the Henon Heiles system till $T = 2000$. (a) The AVF method, (b) The PAVF method, (c) The PAVF-C method, (d) The PAVF-P method.

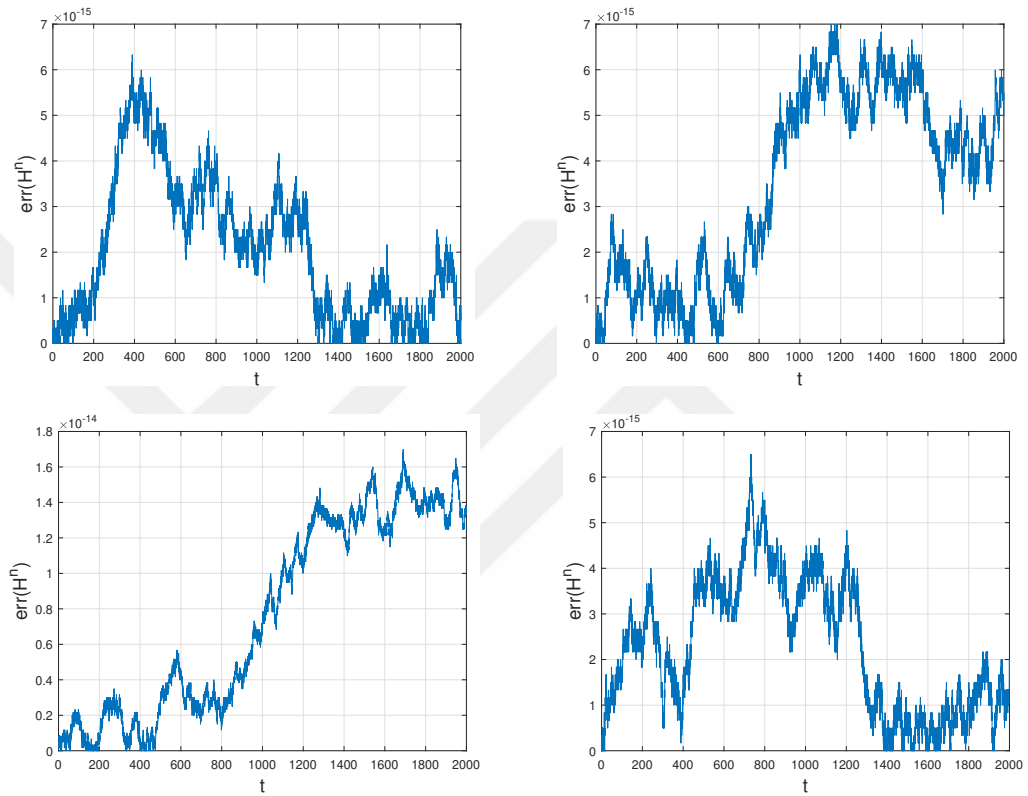


Figure 2.3: Relative errors in energy (2.39) of the four energy preserving methods for the Henon Heiles system till $T = 2000$. (a) The AVF method, (b) The PAVF method, (c) The PAVF-C method, (d) The PAVF-P method.

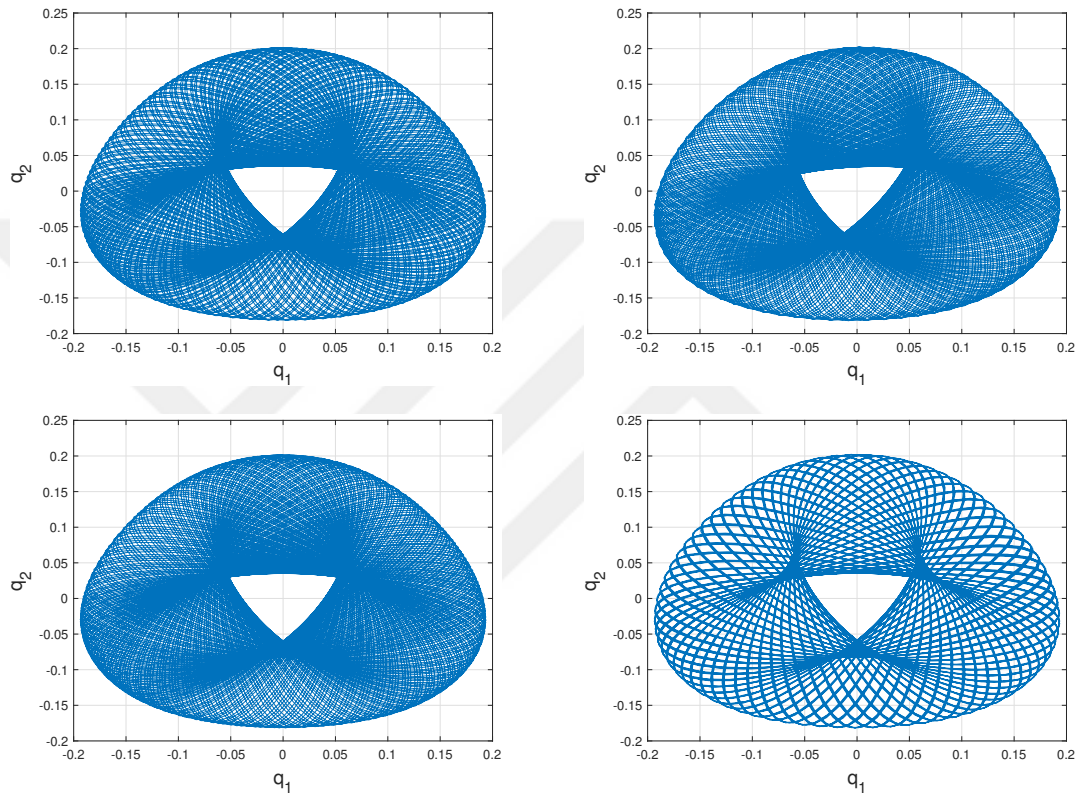


Figure 2.4: Box orbit of the four energy preserving methods for the Henon Heiles system till $T = 1000$. (a) The AVF method, (b) The PAVF method, (c) The PAVF-C method, (d) The PAVF-P method.

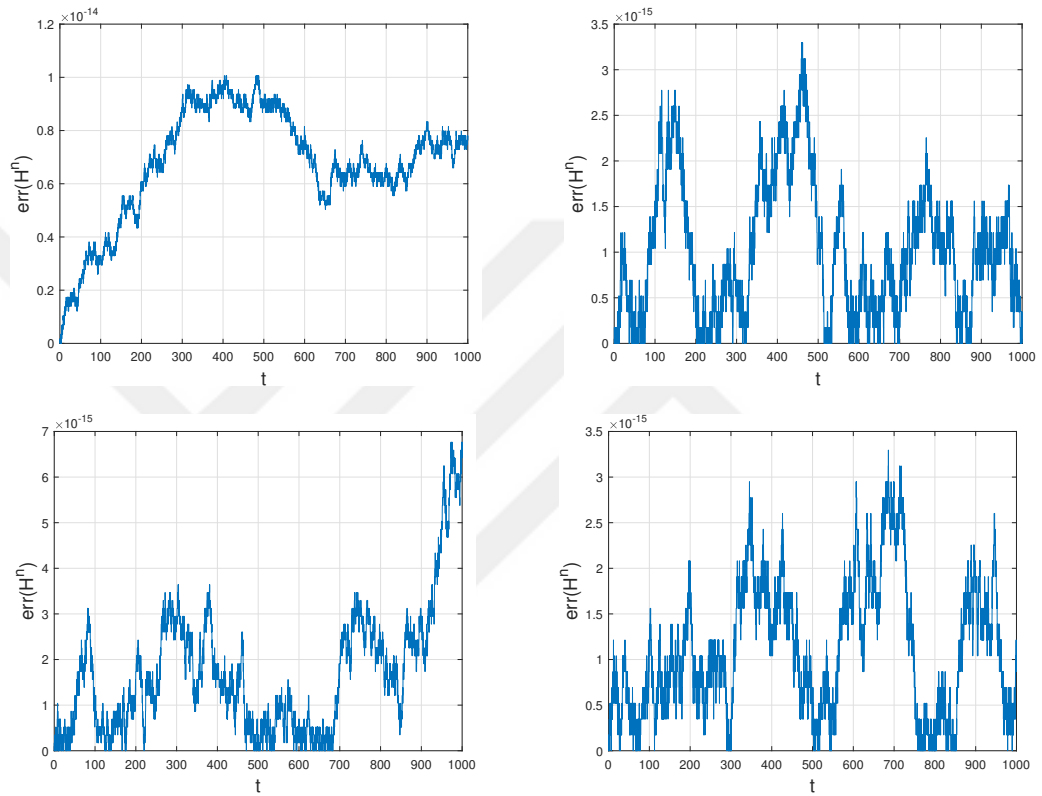


Figure 2.5: Relative errors in energy (2.39) of the four energy preserving methods for the Henon Heiles system till $T = 1000$. (a) The AVF method, (b) The PAVF method, (c) The PAVF-C method, (d) The PAVF-P method.

CHAPTER 3

HAMILTONIAN PARTIAL DIFFERENTIAL EQUATIONS

In this chapter, we begin with some basic definitions and give some examples for Hamiltonian PDE. Then, we give two examples to explain how a Hamiltonian PDE can be discretized to write it in a form of Hamiltonian ODE.

3.1 Introduction

Although the theory and algorithms for Hamiltonian ordinary differential equations (ODEs) are well-developed [34, 52, 53], some difficulties may arise for solving Hamiltonian partial differential equations (PDEs) numerically. This is due to the fact that the underlying phase space is generalized from finite to infinite dimensions. Most popular approaches for treating Hamiltonian PDEs are often via methods of lines in which a PDE is first discretized in space to yield a large system of Hamiltonian ODEs. Then resulting system of ODEs are integrated through a structure preserving numerical method.

Hamiltonian partial differential equations are of the form

$$\frac{\partial u}{\partial t} = \mathcal{J} \frac{\delta \mathcal{H}}{\delta u} \quad (3.1)$$

in the domain $\Omega = (x, t) = \mathbb{R} \times \mathbb{R}$. Here $\mathcal{H} = \int_{\Omega} H(u, u_x, u_{xx}, \dots) dx$ and \mathcal{J} denote the Hamiltonian functional and the skew-adjoint Hamiltonian operator, respectively [6]. The variational derivative is given

$$\frac{\delta \mathcal{H}}{\delta u} = \frac{\partial H}{\partial u} - \frac{\partial}{\partial x} \left(\frac{\partial H}{\partial u_x} \right) + \frac{\partial^2}{\partial x^2} \left(\frac{\partial H}{\partial u_{xx}} \right) - \dots \quad (3.2)$$

Conservation of the energy and other integrals of PDEs play an important role in Hamiltonian PDE. In recent years, several energy or integral preserving methods were developed for ODEs and PDEs by using discrete gradients and discrete variational derivatives [4, 54]. After a suitable spatial discretization of the skew-adjoint operators and Hamiltonian in (3.1), the following finite dimensional Hamiltonian system is obtained:

$$\frac{du}{dt} = J(u) \frac{\partial H}{\partial t} \quad (3.3)$$

Here, $J(u)$ is the $N \times N$ skew-symmetric structure matrix corresponding to the discretization of the skew adjoint operator \mathcal{J} .

Now, we give two examples to explain how an infinite dimensional Hamiltonian can be written as a finite dimensional Hamiltonian system.

3.2 The nonlinear Schrödinger Equation

In this section we will consider the nonlinear Schrödinger equation

$$i\psi_t + \psi_{xx} + a|\psi|^2\psi = 0, \quad (3.4)$$

where $\psi(x, t)$ is complex-valued function, $x \in \mathbb{R}$ and $a > 0$ is a constant parameter. In the soliton theory, this equation is one of the most important completely integrable models arising in many areas of physics fields, including nonlinear optics and plasma.

The nonlinear Schrödinger equation (3.4) can be expressed as an infinite-dimensional Hamiltonian system. Let $p(x, t)$ and $q(x, t)$ be real-valued functions and $\psi = p + iq$. The Hamiltonian formulation of (3.4) can be given as

$$\frac{dz}{dt} = J \frac{\delta \mathcal{H}(z, z_x)}{\delta u} \quad (3.5)$$

where

$$z = (p, q) \quad J = \begin{pmatrix} 0 & 1 \\ -1 & 0 \end{pmatrix}$$

and the Hamiltonian is

$$\mathcal{H}(z, z_x) = \int \frac{1}{2} [p_x^2 + q_x^2 - \frac{a}{2} (p^2 + q^2)^2] dx.$$

The spatial derivatives in (3.5) can be discretized to get a finite-dimensional Hamiltonian system. We assume that the solutions of (3.5) are negligibly small outside an spatial domain $x_L \leq x \leq x_R$. Let

$$P = [p_1, p_2, \dots, p_N]^T, \quad Q = [q_1, q_2, \dots, q_N]^T$$

where N is the number of spatial grid points. Spatial discretization of (3.4) using a central difference approximations yields a semi-discrete system with accuracy $O(\Delta^{2m})$.

$$\frac{d}{dt} \begin{pmatrix} P \\ Q \end{pmatrix} = \begin{pmatrix} 0 & I \\ -I & 0 \end{pmatrix} \begin{pmatrix} M(2m) & 0 \\ 0 & M(2m) \end{pmatrix} \begin{pmatrix} P \\ Q \end{pmatrix} \quad (3.6)$$

where $M(2m)$ is an $N \times N$ matrix and I is $N \times N$ identity matrix. The matrix $M(2m)$ can be written as a sum of two matrices $M(2m) = B(2m) + D$ where

$$D = \text{diag}(-a(p_1^2 + q_1^2), \dots, -a(p_N^2 + q_N^2))$$

is a diagonal matrix. The second-order and fourth-order central difference approximations can be used for spatial discretization. In these two cases we have $M(2) = B(2) + D$ where

$$B(2) = -\frac{1}{\Delta x^2} \begin{pmatrix} -2 & 1 & 0 & \dots & \dots & 0 \\ 1 & -2 & 1 & \dots & \dots & 0 \\ & \ddots & \ddots & \ddots & & \\ & \ddots & \ddots & \ddots & & \\ 0 & 0 & \dots & \dots & -2 & 1 \\ 0 & 0 & \dots & \dots & 1 & -2 \end{pmatrix}$$

and $M(4) = B(4) + D$ where

$$M(4) = -\frac{1}{12\Delta x^2} \begin{pmatrix} -30 & 16 & -1 & 0 & 0 & \dots & \dots & 0 & 0 & 0 \\ 16 & -30 & 16 & -1 & 0 & \dots & \dots & 0 & 0 & 0 \\ -1 & 16 & -30 & 16 & -1 & \dots & \dots & 0 & 0 & 0 \\ & \ddots & \ddots & \ddots & \ddots & \ddots & & & & \\ & & \ddots & \ddots & \ddots & \ddots & \ddots & & & \\ & & & \ddots & \ddots & \ddots & \ddots & \ddots & & \\ & & & & \ddots & \ddots & \ddots & \ddots & \ddots & \\ & & & & & \ddots & \ddots & \ddots & \ddots & \\ 0 & 0 & 0 & \dots & \dots & \dots & \dots & 16 & -30 & 16 \\ 0 & 0 & 0 & \dots & \dots & \dots & \dots & -1 & 16 & -30 \end{pmatrix}.$$

The system (3.6) is a finite dimensional Hamiltonian system. Assume that $Z = (P^T, Q^T)^T$ and

$$J = \begin{pmatrix} 0 & I \\ -I & 0 \end{pmatrix}.$$

Then (3.6) can be rewritten as

$$\frac{dZ}{dt} = J\nabla_z H(Z) \quad (3.7)$$

with the Hamiltonian [55]

$$H(P, Q) = \frac{1}{2}[P^T B(2m)P + Q^T B(2m)Q] - \frac{a}{4} \sum_{i=1}^N (p_i^2 + q_i^2)^2. \quad (3.8)$$

Now, the time derivative in (3.7) can be discretized by any energy preserving scheme such as the AVF scheme or the PAVF scheme.

3.3 The good Boussinesq equation

The "good" Boussinesq equation,

$$W_{tt} = -W_{xxxx} + W_{xx} + (W^2)_{xx} \quad (3.9)$$

is another nonlinear PDE which achieves a balance of dispersion and nonlinearity, resulting in solitons such as the Korteweg de Vries (KdV) and cubic nonlinear Schrödinger equations. It has been demonstrated that the good Boussinesq equation differs from other nonlinear wave equations in that it has a highly complicated solitary wave interaction [56]. Solitary waves exist only for a finite range of velocities, they can merge into a single soliton, and they interact with each other to give rise to anti-solitons. We set $W = u - \frac{1}{2}$ to remove the linear term W_{xx} in Eq.(3.9)

$$u_{tt} = -u_{xxxx} + (u^2)_{xx}. \quad (3.10)$$

We consider the good Boussinesq equation (3.10) in the region $D = [(x, t) \in \mathbb{R}^2 : x_l \leq x \leq x_r, t \geq 0]$ with the initial conditions

$$u(x, t) = f(x), \quad u_t(x, 0) = g(x) \quad (3.11)$$

and the periodic boundary conditions

$$u(x, t) = u(x_r, t), \quad u_x(x_l, t) = u_x(x_r, t). \quad (3.12)$$

The equation (3.10) can be written as an infinite dimensional Hamiltonian system .

Introducing $v_t = -u_{xxx} + (u^2)_x$, we get

$$\begin{pmatrix} u_t \\ v_t \end{pmatrix} = \begin{pmatrix} 0 & \partial_x \\ \partial_x & 0 \end{pmatrix} \begin{pmatrix} \delta\mathcal{H}_u \\ \delta\mathcal{H}_v \end{pmatrix} \quad (3.13)$$

with the Hamiltonian

$$\mathcal{H}(u, v) = \frac{1}{2} \int_{-\infty}^{\infty} (v^2 + \frac{2}{3}u^3 + u_x^2) dx. \quad (3.14)$$

In addition to the Hamiltonian, the momentum $I(u, v) = \int_{-\infty}^{\infty} uv dx$, is the global conserved quantity in the Boussinesq equation. As an infinite-dimensional Hamiltonian system, the Boussinesq equation (3.10), or

$$\begin{aligned} \frac{\partial u}{\partial t} &= \frac{\partial v}{\partial t}, \\ \frac{\partial v}{\partial t} &= -\frac{\partial^3 u}{\partial x^3} + \frac{\partial u^2}{\partial x} \end{aligned} \quad (3.15)$$

is discretized for the spatial derivatives using the second-order central finite-difference approximations. The resulting system Hamiltonian ODEs are given by

$$\begin{aligned} \frac{d}{dt} u_i(t) &= \frac{v_{i+1} - v_{i-1}}{2\Delta x} \\ \frac{d}{dt} v_i(t) &= \frac{u_{i+2} - 2u_{i+1} + 2u_{i-1} - u_{i-2}}{2(\Delta x)^3} + \frac{u_{i+1}^2 - u_{i-1}^2}{2\Delta x} \end{aligned} \quad (3.16)$$

with the Hamiltonian [56]

$$H(u, v) = \frac{1}{2} \sum_{i=1}^N \left[v_i^2 + \frac{2}{3} u_i^3 + \left(\frac{u_{i+1} - u_i}{\Delta x} \right)^2 \right] \quad (3.17)$$

Now, the time derivatives in (3.16) can be discretized by any energy preserving scheme such as the AVF scheme or the PAVF scheme.

3.4 Klein-Gordon Schrödinger Equation

In this section, we will review some material from [1]. The Klein–Gordon–Schrödinger (KGS) equation

$$\begin{aligned} i\varphi_t + \frac{1}{2}\varphi_{xx} + u\varphi &= 0, \\ u_{tt} - u_{xx} + u - |\varphi|^2 &= 0 \end{aligned} \quad (3.18)$$

where $x \in (x_L, x_R)$, $t > 0$ is a system of conserved scalar nucleons interacting with neutral scalar Mesons coupled with Yukawa interaction. In (3.18) $\varphi(x, t)$ denotes a complex scalar nucleon field and $u(x, t)$ denotes a real scalar meson field. [12, 13]. Decomposing the real and imaginary parts of the complex valued function $\varphi = q + pi$ and introducing $v = \frac{1}{2}u_t$, the equation (3.18) can be rewritten as a first-order system of equations

$$\begin{aligned} u_t &= 2v, \\ v_t &= \frac{1}{2}(u_{xx} - u + (p^2 + q^2)), \\ p_t &= \frac{1}{2}q_{xx} + uq, \\ q_t &= -\frac{1}{2}p_{xx} - up. \end{aligned} \tag{3.19}$$

We consider the homogeneous Dirichlet boundary conditions $p(x_L, t) = p(x_R, t) = 0$, $q(x_L, t) = q(x_R, t) = 0$, $u(x_L, t) = u(x_R, t) = 0$, $v(x_L, t) = v(x_R, t) = 0$. The system (3.19) can be written as an infinite dimensional Hamiltonian PDE

$$\frac{dz}{dt} = J \frac{\delta H(z)}{\delta z} \tag{3.20}$$

where

$$z = (u, v, p, q)^T, J = \begin{bmatrix} 0 & 1 & 0 & 0 \\ -1 & 0 & 0 & 0 \\ 0 & 0 & 0 & -1 \\ 0 & 0 & 1 & 0 \end{bmatrix}$$

and the Hamiltonian is defined by

$$\mathcal{H}(z) = \int_{x_L}^{x_R} \frac{1}{4} [p_x^2 + q_x^2 + u^2 + u_x^2 + 4v^2 - 2u(p^2 + q^2)] dx.$$

Besides the energy conservation $H(z(t)) = H(z(0))$, the KGS system (3.19) has also mass conservation [1]

$$M(z(t)) = \int_{x_L}^{x_R} (p^2 + q^2) dx = M(z(0)).$$

3.4.1 Energy preserving AVF and PAVF schemes for Klein-Gordon Schrödinger equation

First, we consider a conventional spatial discretization process so the resulting semi-discrete system can be written as a finite dimensional Hamiltonian system. The spatial

derivatives in (3.19) are approximated using the second order central difference operator. Let $t_n = n\tau$, for $n = 0, 1, \dots$, and $x_j = x_L + jh$, for $j = 0, 1, \dots, J$ where $h = \frac{L}{J}$ and τ are the temporal and spatial step sizes, respectively. Let $(u_j^n, v_j^n, p_j^n, q_j^n)$ be the numerical approximations corresponding to the exact solution $(u(x, t), v(x, t), p(x, t), q(x, t))$ at the grid point (x_j, t_n) . The corresponding vector forms are indicated at any time level by $U = (u_0, u_1, \dots, u_j)^T$, $V = (v_0, v_1, \dots, v_j)^T$, $P = (p_0, p_1, \dots, p_j)^T$, $Q = (q_0, q_1, \dots, q_j)^T$.

$$(U, V) = h \sum_{j=0}^J u_j v_j, \quad \|U\|_j = (U, U)^{\frac{1}{2}}, \quad \|U\|_\infty = \max_j |u_j|$$

are the standard inner product and the vector norms. Discretization of spatial derivatives in the KGS system (3.19) by using the second-order central difference approximation yields the semi-discrete system

$$\begin{aligned} U_t &= 2V \\ V_t &= \frac{1}{2}DU - \frac{1}{2}U + \frac{1}{2}(P \cdot P + Q \cdot Q) \\ P_t &= \frac{1}{2}DQ + U \cdot Q \\ Q_t &= -\frac{1}{2}DP - U \cdot P \end{aligned} \tag{3.21}$$

where D is the matrix corresponding to the second-order central difference discretization and $\cdot \cdot$ is the element multiplication of vectors, i.e. $P \cdot Q = (p_0 q_0, p_1 q_1, \dots, p_J q_J)^T$. Thus the system (3.21) is in a finite dimensional Hamiltonian system of the form

$$\frac{dZ}{dt} = f(Z) = S \nabla H(Z) \tag{3.22}$$

where

$$z = (U^T, V^T, P^T, Q^T)^T, S = \begin{bmatrix} 0 & I & 0 & 0 \\ -I & 0 & 0 & 0 \\ 0 & 0 & 0 & -I \\ 0 & 0 & I & 0 \end{bmatrix}$$

and

$$H(Z) = \frac{1}{4} \left(-P^T DP - Q^T DQ - U^T DU + U^T U + 4V^T V - 2U^T (P \cdot P + Q \cdot Q) \right).$$

Now, the time derivatives in (3.22) can be discretized by any energy preserving scheme such as the AVF scheme or the PAVF scheme.

We can consider to construct the AVF method for (3.22). Applying the AVF method

to the system (3.22) yields

$$\begin{aligned}
\delta_t^+ U^n &= V^n + V^{n+1} \\
\delta_t^+ V^n &= \frac{1}{2}(DU^{n+\frac{1}{2}} - U^{n+\frac{1}{2}}) + \frac{1}{12}((P^{n+1})^2 + 4(P^{n+\frac{1}{2}})^2 + (P^n)^2 \\
&\quad + (Q^{n+1})^2 + 4(Q^{n+\frac{1}{2}})^2 + (Q^n)^2) \\
\delta_t^+ P^n &= \frac{1}{2}DQ^{n+\frac{1}{2}} + \frac{1}{6}(U^{n+1} \cdot Q^{n+1} + 4U^{n+\frac{1}{2}} \cdot Q^{n+\frac{1}{2}} + U^n \cdot Q^n) \\
\delta_t^+ Q^n &= -\frac{1}{2}DP^{n+\frac{1}{2}} - \frac{1}{6}(U^{n+1} \cdot P^{n+1} + 4U^{n+\frac{1}{2}} \cdot P^{n+\frac{1}{2}} + U^n \cdot P^n)
\end{aligned} \tag{3.23}$$

where δ_t^+ is the forward differentiation operator. It is clear that the system (3.23) is fully implicit. The PAVF scheme for the KGS system (3.18) can be given as

$$\begin{aligned}
\delta_t^+ U^n &= \int_0^1 H_v(U^{n+1}, \xi V^{n+1} + (1-\xi)V^n, P^n, Q^n) d\xi, \\
\delta_t^+ V^n &= -\int_0^1 H_u(\xi U^{n+1} + (1-\xi)U^n, V^n, P^n, Q^n) d\xi, \\
\delta_t^+ Q^n &= -\int_0^1 H_Q(U^{n+1}, V^{n+1}, P^{n+1}, \xi Q^{n+1} + (1-\xi)Q^n) d\xi, \\
\delta_t^+ P^n &= -\int_0^1 H_P(U^{n+1}, V^{n+1}, \xi P^{n+1} + (1-\xi)P^n, Q^n) d\xi,
\end{aligned} \tag{3.24}$$

or explicitly written as

$$\begin{aligned}
\delta_t^+ U^n &= V^n + V^{n+1} \\
\delta_t^+ V^n &= \frac{1}{2}(DU^{n+\frac{1}{2}} - U^{n+\frac{1}{2}} + (P^n)^2 + (Q^n)^2), \\
\delta_t^+ P^n &= \frac{1}{2}DQ^{n+\frac{1}{2}} + U^{n+\frac{1}{2}} \cdot Q^{n+\frac{1}{2}}, \\
\delta_t^+ Q^n &= -\frac{1}{2}DP^{n+\frac{1}{2}} - U^{n+1} \cdot P^{n+\frac{1}{2}}.
\end{aligned} \tag{3.25}$$

Obviously, the PAVF scheme (3.25) requires to solve two set of linear equations and does not require any iterative solver. First two equations in (3.25) can be solved for U^{n+1} and V^{n+1} , then these solutions can be used to find P^{n+1} and Q^{n+1} in the last two equations in (3.25). When we compare the AVF scheme (3.23) with the PAVF scheme (3.25), we see that the PAVF scheme is simpler than the AVF scheme.

Theorem 3.4.1 [1] *In addition to energy conservation, PAVF (3.25) is also a mass-conservative*

$$M(U^n, V^n, P^n, Q^n) = M(U^0, V^0, P^0, Q^0), \quad n = 1, 2, \dots$$

Proof. Multiplying the last two equations in (3.25) by $P^{n+1} + P^n$ and $Q^{n+1} + Q^n$, respectively, we get

$$\frac{h}{\tau}(P^{n+1} + P^n)^T(P^{n+1} - P^n) = h(P^{n+1} + P^n)^T\left(\frac{1}{2}DQ^{n+\frac{1}{2}} + U^{n+\frac{1}{2}} \cdot Q^{n+\frac{1}{2}}\right), \tag{3.26}$$

and

$$\frac{h}{\tau}(Q^{n+1} + Q^n)^T(Q^{n+1} - Q^n) = h(Q^{n+1} + Q^n)^T\left(\frac{1}{2}DP^{n+\frac{1}{2}} + U^{n+1} \cdot P^{n+\frac{1}{2}}\right). \quad (3.27)$$

Summing (3.26) and (3.27), we obtain the mass conservation

$$\frac{1}{\tau}(\|P^{n+1}\|_J^2 + \|Q^{n+1}\|_J^2 - \|P^n\|_J^2 - \|Q^n\|_J^2) = 0. \quad (3.28)$$

□

Now we present the adjoint method of the PAVF

$$\begin{aligned} \delta_t^+ U^n &= V^n + V^{n+1} \\ \delta_t^+ V^n &= \frac{1}{2}(DU^{n+\frac{1}{2}} - U^{n+\frac{1}{2}} + (P^{n+1})^2 + (Q^{n+1})^2) \\ \delta_t^+ P^n &= \frac{1}{2}DQ^{n+\frac{1}{2}} + U^n \cdot Q^{n+\frac{1}{2}} \\ \delta_t^+ Q^n &= -\frac{1}{2}DP^{n+\frac{1}{2}} - U^n \cdot P^{n+\frac{1}{2}} \end{aligned} \quad (3.29)$$

for the KGS system (3.22). Energy and mass conservation of the adjoint method (3.29) can shown similarly. Using the adjoint scheme (3.29), the corresponding PAVF-C scheme can be written as

$$\begin{aligned} \frac{1}{\tau}(U^* - U^n) &= V^n + V^*, \\ \frac{1}{\tau}(V^* - V^n) &= \frac{1}{4}(D(U^* + U^n) - (U^* + U^n) + 2(P^n)^2 + 2(Q^n)^2), \\ \frac{1}{\tau}(P^* - P^n) &= \frac{1}{4}D(Q^* + Q^n) + \frac{1}{2}U^* \cdot (Q^* + Q^n), \\ \frac{1}{\tau}(Q^* - Q^n) &= \frac{1}{4}D(P^* + P^n) - \frac{1}{2}U^* \cdot (P^* + P^n), \\ \frac{1}{\tau}(U^{n+1} - U^*) &= V^{n+1} + V^*, \\ \frac{1}{\tau}(V^{n+1} - V^*) &= \frac{1}{4}(D(U^* + U^{n+1}) - (U^* + U^{n+1}) + 2(P^{n+1})^2 + 2(Q^{n+1})^2), \\ \frac{1}{\tau}(P^{n+1} - P^*) &= \frac{1}{4}D(Q^* + Q^{n+1}) + \frac{1}{2}U^* \cdot (Q^* + Q^{n+1}), \\ \frac{1}{\tau}(Q^{n+1} - Q^*) &= -\frac{1}{4}D(P^* + P^{n+1}) - \frac{1}{2}U^* \cdot (P^* + P^{n+1}). \end{aligned} \quad (3.30)$$

Analogously, the PAVF-P scheme is

$$\begin{aligned} \delta_t^+ U^n &= V^n + V^{n+1}, \\ \delta_t^+ V^n &= \frac{1}{2}(DU^{n+\frac{1}{2}} - U^{n+\frac{1}{2}}) + \frac{1}{4}((P^n)^2 + (Q^n)^2 + (P^{n+1})^2 + (Q^{n+1})^2), \\ \delta_t^+ P^n &= \frac{1}{2}DQ^{n+\frac{1}{2}} + U^{n+\frac{1}{2}} \cdot Q^{n+\frac{1}{2}}, \\ \delta_t^+ Q^n &= -\frac{1}{2}DP^{n+\frac{1}{2}} - U^{n+\frac{1}{2}} \cdot P^{n+\frac{1}{2}}. \end{aligned} \quad (3.31)$$

3.5 Zakharov System

In this section, we will consider the Zakharov equation which has many applications in physics for example in deep-water wave theory [22], communication [23], non-linear pulse propagation in fibers [24], optical systems [25, 26, 27], superfluids [28], and plasma [29, 30]. The interaction between Langmuir and ion acoustic waves in a plasma is described by the Zakharov system of equations [2]

$$\begin{aligned} i\partial_t\phi + \partial_{xx}\phi + 2\phi\psi &= 0 \\ \partial_{tt} - \partial_{tt}\psi + \partial_{xx}(|\phi|^2) &= 0 \end{aligned} \quad (3.32)$$

where the complex valued function $\phi(x, t)$ is the slowly varying envelope of the highly oscillatory electric field and $\psi(x, t)$ is the real valued function which represents the fluctuation of an ion density about its equilibrium value. The exact Langmuir soliton solution of the equation (3.32) is given by

$$\begin{aligned} \phi(x, t, x_0, B, c) &= Bi \sqrt{1 - c^2} \operatorname{sech}(2B(x - x_0 - ct)) \\ &\quad \times \exp\left(i\left(\frac{c(x-x_0)}{2} - (c^2/4 - 4B^2)t\right)\right) \\ \psi(x, t, x_0, B, c) &= 4B^2 \operatorname{sech}^2(2B(x - x_0 - ct)) \end{aligned} \quad (3.33)$$

where B , c and x_0 are constants and $i^2 = -1$. These are the solitary waves initially located at the spatial position x_0 , and moving to the right with the velocity c . The global existence of a weak solution and the existence and uniqueness of the smooth solution of the Zakharov system in one-dimension are proven in [15]. On the other hand, numerical studies for the Zakharov system (3.32) is rare. Recently, the multi-symplectic integration [9], time-splitting spectral methods [8] and conservative finite difference schemes [57] for the Zakharov system (3.32) is considered. We consider the Zakharov system (3.32) with initial conditions

$$\phi_0(x) = \phi(x, 0, x_0, B, c), \psi_0(x) = \psi(x, 0, x_0, B, c), \psi_1(x) = \partial_t(x, t, x_0, B, c)|_{t_0} \quad (3.34)$$

and the periodic boundary conditions

$$\phi(x_L, t, x_0, B, c) = \phi(x_R, t, x_0, B, c) \quad \psi(x_L, t, x_0, B, c) = \psi(x_R, t, x_0, B, c). \quad (3.35)$$

Converting the system into a finite dimensional Hamiltonian system, we will propose energy preserving and mass preserving numerical methods.

3.5.1 Energy preserving AVF and PAVF schemes for Zakharov system

We start with the infinite dimensional Hamiltonian structure of the Zakharov system (3.32) [9]. Let u, v, p and q are real functions and introduce $\phi = u + iv, \partial_t \phi = p + iq$ and $\partial_{xx} f = \partial_t \psi$. Then (3.32) can be written as

$$\begin{aligned}\partial_t u &= -\partial_{xx} v - 2v\psi, \\ \partial_t v &= \partial_{xx} u + 2u\psi, \\ \partial_t \psi &= \partial_{xx} f, \\ \partial_t f &= \psi - (u^2 + v^2).\end{aligned}\tag{3.36}$$

The infinite-dimensional Hamiltonian form of (3.32) is written as

$$\partial_t z = J \frac{\delta H}{\delta z}\tag{3.37}$$

where

$$z = (u, v, \psi, f)^T \quad J = \begin{pmatrix} J_1 & 0 \\ 0 & J_1 \end{pmatrix}, \quad J_1 = \begin{pmatrix} 0 & 1 \\ -1 & 0 \end{pmatrix}$$

and

$$\mathcal{H} = \int_{x_L}^{x_R} \frac{1}{2} [(\partial_x u)^2 + (\partial_x v)^2 + \psi^2 + (\partial_x f)^2 - 2\psi(u^2 + v^2)] dx\tag{3.38}$$

Theorem 3.5.1 [9] *The Zakharov equation (3.32) preserves the energy*

$$\frac{d}{dt} \mathcal{H}(z) = 0, \quad \text{i.e. } \mathcal{H}(z(t)) = \mathcal{H}(z(0)).\tag{3.39}$$

Theorem 3.5.2 *The Zakharov equation (3.32) obeys the mass conservation*

$$M(z(t)) = \int_{x_L}^{x_R} (U^2 + V^2) dx = M(z(0))\tag{3.40}$$

Proof.

$$\begin{aligned}\frac{d}{dt} M(z(t)) &= \frac{d}{dt} \int_{x_L}^{x_R} (U^2 + V^2) dx = 2 \int_{x_L}^{x_R} (UU_t + VV_t) dx \\ &= 2 \int_{x_L}^{x_R} [U(-V_{xx} - 2V\psi) + V(U_{xx} + 2U\psi)] dx \\ &= 2 \int (-UV_{xx} + VU_{xx}) dx \\ &= 2 \int_{x_L}^{x_R} \frac{\partial}{\partial x} (U_x V - V_x U) dx \\ &= 2(U_x V - V_x U)|_{x_L}^{x_R} = 0.\end{aligned}\tag{3.41}$$

□

In order to process the numerical discretization, we introduce a uniform grid $(x_j, t_n) \in R \times R$ with mesh-length $\Delta x = h$ in the x -direction and mesh-length $\Delta t = \tau$ in the t -direction. The spatial interval $[x_L, x_R]$ is divided into N equal subintervals with grid spacing $h = (x_R - x_L)/N$. We denote by u_j, v_j, ψ_j, f_j the approximation to $u(x, t), v(x, t), \psi(x, t), f(x, t)$ respectively. The second-order spatial derivatives ∂_{xx} in (3.36) are discretized by using the second-order central difference approximation and get the semi-discrete system

$$\begin{aligned}\frac{d}{dt}u_j &= -\frac{v_{j+1} - 2v_j + v_{j-1}}{h^2} - 2v_j\psi_j, \\ \frac{d}{dt}v_j &= \frac{u_{j+1} - 2u_j + u_{j-1}}{h^2} + 2j\psi_j, \\ \frac{d}{dt}\psi_j &= \frac{f_{j+1} - 2f_j + f_{j-1}}{h^2}, \\ \frac{d}{dt}f_j &= \psi_j - (u_j^2 + v_j^2).\end{aligned}\tag{3.42}$$

The system (3.42) can be written as a finite dimensional Hamiltonian system

$$\frac{d}{dt}Z_j = J\nabla H(z_j)\tag{3.43}$$

with $Z_j = (u_j, v_j, \psi_j, f_j)^T$ and

$$J = \begin{bmatrix} 0 & I & 0 & 0 \\ -I & 0 & 0 & 0 \\ 0 & 0 & 0 & -I \\ 0 & 0 & I & 0 \end{bmatrix}.$$

Here, I is the $N \times N$ identity matrix

$$H(Z) = \sum_{j=1}^N \frac{1}{2} [(\delta_x u_j)^2 + (\delta_x v_j)^2 + (\delta_x f_j)^2 + \psi^2 - 2\psi_j(u_j^2 + v_j^2)]$$

where $\delta_x u_j = \frac{u_{j+1} - u_j}{h}$, $\delta_x v_j = \frac{v_{j+1} - v_j}{h}$, $\delta_x f_j = \frac{f_{j+1} - f_j}{h}$.

The second-order AVF method for (3.42) is written as

$$\begin{aligned}\delta_t^+ u^n &= -Dv^{n+1/2} - \frac{2}{3}[v^{n+1}\psi^{n+1} + \frac{1}{2}v^{n+1}\psi^n + \frac{1}{2}v^n\psi^{n+1} + v^n\psi^n], \\ \delta_t^+ v^n &= Du^{n+1/2} - \frac{2}{3}[u^{n+1}\psi^{n+1} + \frac{1}{2}u^{n+1}\psi^n + \frac{1}{2}u^n\psi^{n+1} + u^n\psi^n], \\ \delta_t^+ \psi^n &= Df^{n+1/2}, \\ \delta_t^+ f^n &= \psi^{n+1/2} - \frac{1}{3}[(u^{n+1})^2 + u^{n+1}u^n + (u^n)^2] - \frac{1}{3}[(v^{n+1})^2 + v^{n+1}v^n + (v^n)^2],\end{aligned}\tag{3.44}$$

where $\delta_t^+ u^n = \frac{u^{n+1}-u^n}{\tau}$, $\delta_t^+ v^n = \frac{v^{n+1}-v^n}{\tau}$, $\delta_t^+ \psi^n = \frac{\psi^{n+1}-\psi^n}{\tau}$, $\delta_t^+ f^n = \frac{f^{n+1}-f^n}{\tau}$ and D is the central operator corresponding to the spatial second order central difference approximation. The PAVF method for (3.42) is

$$\begin{aligned}\delta_t^+ u^n &= -Dv^{n+1/2} - (v^{n+1} + v^n)\psi^n, \\ \delta_t^+ v^n &= Du^{n+1/2} + (u^{n+1} + u^n)\psi^n, \\ \delta_t^+ \psi^n &= Df^{n+1/2}, \\ \delta_t^+ f^n &= \psi^{n+1/2} - [(u^{n+1})^2 + (v^{n+1})^2],\end{aligned}\tag{3.45}$$

and the adjoint PAVF method for (3.42) is

$$\begin{aligned}\delta_t^+ u^n &= -Dv^{n+1/2} - (v^{n+1} + v^n)\psi^{n+1}, \\ \delta_t^+ v^n &= Du^{n+1/2} + (u^{n+1} + u^n)\psi^{n+1}, \\ \delta_t^+ \psi^n &= Df^{n+1/2}, \\ \delta_t^+ f^n &= \psi^{n+1/2} - [(u^n)^2 + (v^n)^2].\end{aligned}\tag{3.46}$$

Theorem 3.5.3 *The PAVF (3.45) for the Zakharov equation is mass-conservative in the sense that*

$$M(u^n, v^n, \psi^n, f^n) = M(u^0, v^0, \psi^0, f^0), \quad n = 1, 2, \dots$$

Proof. Multiplying the first two equations in (3.45) by $(u^{n+1} + u^n)^T$ and $(v^{n+1} + v^n)^T$, respectively, we get

$$\frac{1}{\tau}(u^{n+1} + u^n)^T(u^{n+1} - u^n) = (u^{n+1} + u^n)^T \left(-Dv^{n+1/2} - (v^{n+1} + v^n)\psi^n \right),\tag{3.47}$$

and

$$\frac{1}{\tau}(v^{n+1} + v^n)^T(v^{n+1} - v^n) = (v^{n+1} + v^n)^T \left(Du^{n+1/2} + (u^{n+1} + u^n)\psi^n \right).\tag{3.48}$$

Summing (3.47) and (3.48), we obtain the mass conservation

$$\frac{1}{\tau}(\|u^{n+1}\|_J^2 + \|v^{n+1}\|_J^2 - \|u^n\|_J^2 - \|v^n\|_J^2) = 0.\tag{3.49}$$

This completes the proof. □

Using the PAVF method for Zakharov system with its adjoint method, the second-order energy preserving PAVF-C method for Zakharov system can be written as

$$\begin{aligned}
\frac{2}{\tau}(u^* - u^n) &= -\frac{D}{2}(v^* + v^n) - (v^* + v^n)\psi^n \\
\frac{2}{\tau}(v^* - v^n) &= \frac{D}{2}(u^* + u^n) + (u^* + u^n)\psi^n \\
\frac{2}{\tau}(\psi^* - \psi^n) &= \frac{D}{2}(f^* + f^n) \\
\frac{2}{\tau}(f^* - f^n) &= \frac{1}{2}(\psi^* + \psi^n) - [(u^*)^2 + (v^*)^2] \\
\frac{2}{\tau}(u^{n+1} - u^*) &= -\frac{D}{2}(v^{n+1} + v^*) - (v^{n+1} + v^*)\psi^{n+1} \\
\frac{2}{\tau}(v^{n+1} - v^*) &= \frac{D}{2}(u^{n+1} + u^*) + (u^{n+1} + u^*)\psi^{n+1} \\
\frac{2}{\tau}(\psi^{n+1} - \psi^*) &= \frac{D}{2}(f^{n+1} + f^*) \\
\frac{2}{\tau}(f^{n+1} - f^*) &= \frac{1}{2}(\psi^{n+1} + \psi^*) - [(u^*)^2 + (v^*)^2]
\end{aligned} \tag{3.50}$$

In addition, the second-order energy preserving PAVF-P method can be written as

$$\begin{aligned}
\delta_t^+ u^n &= -Dv^{n+1/2} - \frac{1}{2}(v^{n+1} + v^n)(\psi^n + \psi^{n+1}) \\
\delta_t^+ v^n &= Du^{n+1/2} + \frac{1}{2}(u^{n+1} + u^n)(\psi^n + \psi^{n+1}) \\
\delta_t^+ \psi^n &= Df^{n+1/2} \\
\delta_t^+ f^n &= \frac{1}{2}(\psi^{n+1} + \psi^n) - \frac{1}{2}[(u^{n+1})^2 + (v^{n+1})^2 + (u^n)^2 + (v^n)^2]
\end{aligned} \tag{3.51}$$

3.5.2 Numerical Experiments

In order to show the accuracy and the rate of convergency for the new energy preserving schemes AVF (3.44), PAVF (3.45), PAVF-C (3.50) and PAVF-P (3.51), we use the errors

$$\begin{aligned}
L_\infty(\phi, \Delta x, \Delta t) &= \max_{1 \leq j \leq N} |\phi(x_j, t_n) - \phi_j^n| \\
L_\infty(\psi, \Delta x, \Delta t) &= \max_{1 \leq j \leq N} |\psi(x_j, t_n) - \psi_j^n| \\
L_2(\phi, \Delta x, \Delta t) &= \left(\Delta x \sum_{j=1}^N |\phi(x_j, t_n) - \phi_j^n|^2 \right)^{1/2} \\
L_2(\psi, \Delta x, \Delta t) &= \left(\Delta x \sum_{j=1}^N |\psi(x_j, t_n) - \psi_j^n|^2 \right)^{1/2}
\end{aligned} \tag{3.52}$$

where $\phi(x_j, t_n), \psi(x_j, t_n)$ are exact solutions and ϕ_j^n, ψ_j^n are approximate solution at the point (x_j, t_n) . The rate of convergence is obtained by using

$$\text{order} \approx \ln(L_\infty(z, \Delta x_1, \Delta t_1)/L_\infty(z, \Delta x_2, \Delta t_2)) / \ln(\Delta t_1/\Delta t_2)$$

for temporal order and

$$\text{order} \approx \ln(L_\infty(z, \Delta x_1, \Delta t_1)/L_\infty(z, \Delta x_2, \Delta t_2)) / \ln(\Delta x_1/\Delta x_2)$$

for spatial order. Here z is either ϕ and ψ . The relative discrete Hamiltonian energy error and the discrete mass error of the Zakharov equation is defined as

$$R_H(t) = \left| \frac{H(Z^n) - H(Z^0)}{H(Z^0)} \right|, \quad R_M(t) = \left| \frac{M(Z^n) - M(Z^0)}{M(Z^0)} \right| \quad (3.53)$$

where $H(Z^n)$ and $M(Z^n)$ are the discrete Hamiltonian and mass at time $t_n = n\Delta t$ and $H(Z^0)$ and $M(Z^0)$ are the initial discrete Hamiltonian and the mass, respectively. The initial conditions are taken as

$$\begin{aligned} \phi_0(x) &= \phi(x, 0, x_0, B, c) \\ \psi_0(x) &= \psi(x, 0, x_0, B, c) \\ \psi_1(x) &= \partial_t \psi(x, t, x_0, B, c)|_{t=0}. \end{aligned} \quad (3.54)$$

To demonstrate the long time behaviour of the energy preserving schemes we take periodic boundary conditions

$$\phi(x_L, t) = \phi(x_R, t) \quad \psi(x_L, t) = \psi(x_L, t)$$

in all experiments. First, we set the space interval $x \in [-15, 15]$ with parameters $c = 0.1, x_0 = 0$, and $B = 0.5$. Tables 3.1 - 3.4 show the errors and the order of accuracy in time for the four energy preserving schemes. We choose $\Delta x = 0.01$ small enough so that the error that comes from the spatial discretization is negligible compared to the temporal discretization error. We find that all the methods are second order in time except the PAVF method which is only first order accuracy in time. The similar results are obtained in [1]. Tables 3.5 - 3.8 show the errors and the order of accuracy in space for the four energy preserving schemes. We choose $\Delta t = 0.01$ small enough so that the error that comes from the temporal discretization is negligible compared to the spatial discretization error. As expected, all the methods are second order in space. The accuracy test validates the correctness of our methods AVF (3.44), PAVF (3.45), PAVF-C (3.50) and PAVF-P (3.51).

Table 3.1: Temporal accuracy for the energy preserving AVF method with $T = 10$ and $N = 256$

τ	$L_\infty(\phi)$	order	$L_2(\phi)$	order
0.01	$2.5799e - 02$	$3.8091e - 02$
0.005	$2.5834e - 02$	2.00	$3.8149e - 02$	2.00
0.004	$2.5840e - 02$	2.00	$3.8158e - 02$	2.00
0.003	$2.5845e - 02$	2.00	$3.8166e - 02$	2.00
τ	$L_\infty(\Psi)$	order	$L_2(\Psi)$	order
0.01	$4.5365e - 02$	$5.7290e - 02$
0.005	$4.5400e - 02$	2.00	$5.7362e - 02$	2.00
0.004	$4.5405e - 02$	2.00	$5.7372e - 02$	2.00
0.003	$4.5408e - 02$	2.00	$5.7382e - 02$	2.00

Table 3.2: Temporal accuracy for the energy and the mass preserving PAVF method with $T = 10$ and $N = 256$

τ	$L_\infty(\phi)$	order	$L_2(\phi)$	order
0.01	$2.7004e - 02$	$3.9996e - 02$
0.005	$2.6422e - 02$	1.00	$3.9074e - 02$	1.00
0.004	$2.6308e - 02$	1.00	$3.8893e - 02$	1.00
0.003	$2.6194e - 02$	1.00	$3.8714e - 02$	1.00
τ	$L_\infty(\Psi)$	order	$L_2(\Psi)$	order
0.01	$4.5358e - 02$	$5.7426e - 02$
0.005	$4.5372e - 02$	1.00	$5.7396e - 02$	1.00
0.004	$4.5378e - 02$	1.00	$5.7394e - 02$	1.00
0.003	$4.5386e - 02$	1.00	$5.7394e - 02$	1.00

Table 3.3: Temporal accuracy for the energy and the mass preserving PAVF-C method with $T = 10$ and $N = 256$

τ	$L_\infty(\phi)$	order	$L_2(\phi)$	order
0.01	$2.5826e - 02$	$3.8137e - 02$
0.005	$2.5842e - 02$	2.00	$3.8160e - 02$	2.00
0.004	$2.5845e - 02$	2.00	$3.8165e - 02$	2.00
0.003	$2.5848e - 02$	2.00	$3.8170e - 02$	2.00
τ	$L_\infty(\Psi)$	order	$L_2(\Psi)$	order
0.01	$4.5406e - 02$	$5.7353e - 02$
0.005	$4.5410e - 02$	2.00	$5.7377e - 02$	2.00
0.004	$4.5411e - 02$	2.00	$5.7382e - 02$	2.00
0.003	$4.5412e - 02$	2.00	$5.7387e - 02$	2.00

Table 3.4: Temporal accuracy for the energy and the mass preserving PAVF-P method with $T = 10$ and $N = 256$

τ	$L_\infty(\phi)$	order	$L_2(\phi)$	order
0.01	$2.5827e - 02$	$3.8136e - 02$
0.005	$2.5841e - 02$	2.00	$3.8161e - 02$	2.00
0.004	$2.5844e - 02$	2.00	$3.8166e - 02$	2.00
0.003	$2.5848e - 02$	2.00	$3.8171e - 02$	2.00
τ	$L_\infty(\Psi)$	order	$L_2(\Psi)$	order
0.01	$4.5408e - 02$	$5.7354e - 02$
0.005	$4.5411e - 02$	2.00	$5.7378e - 02$	2.00
0.004	$4.5412e - 02$	2.00	$5.7383e - 02$	2.00
0.003	$4.5412e - 02$	2.00	$5.7387e - 02$	2.00

Table 3.5: Spatial accuracy for the energy preserving PAVF method with $\Delta t = 0.01$

Δx	$L_\infty(\phi)$	order	$L_2(\phi)$	order
0.1	$4.0076e - 03$	$5.3108e - 03$
0.2	$9.8568e - 04$	2.00	$1.3150e - 03$	2.00
0.05	$2.4614e - 04$	2.00	$3.2633e - 04$	2.00
Δx	$L_\infty(\Psi)$	order	$L_2(\Psi)$	order
0.1	$7.7833e - 03$	$7.4923e - 03$
0.2	$1.9467e - 03$	2.00	$1.8585e - 03$	2.00
0.05	$4.8151e - 04$	2.00	$4.6230e - 04$	2.00

Table 3.6: Spatial accuracy for the energy and the mass preserving PAVF method with $\Delta t = 0.01$

Δx	$L_\infty(\phi)$	order	$L_2(\phi)$	order
0.2	$4.3062e - 03$	$6.0712e - 03$
0.1	$1.7209e - 03$	2.00	$2.3418e - 03$	2.00
0.05	$1.1597e - 03$	2.00	$1.6257e - 03$	2.00
Δx	$L_\infty(\Psi)$	order	$L_2(\Psi)$	order
0.01	$7.9353e - 03$	$7.6183e - 03$
0.005	$2.3176e - 03$	2.00	$2.1772e - 03$	2.00
0.004	$1.0512e - 03$	2.00	$1.2006e - 03$	2.00

Table 3.7: Spatial accuracy for the energy and the mass preserving PAVF-C method with $\Delta t = 0.01$

Δx	$L_\infty(\phi)$	order	$L_2(\phi)$	order
0.2	$4.0095e - 03$	$5.3140e - 03$
0.1	$9.8752e - 04$	2.00	$1.3181e - 03$	2.00
0.05	$2.4791e - 04$	2.00	$3.2945e - 04$	2.00
Δx	$L_\infty(\Psi)$	order	$L_2(\Psi)$	order
0.1	$7.7887e - 03$	$7.4958e - 03$
0.2	$1.9520e - 03$	2.00	$1.8617e - 03$	2.00
0.05	$4.8679e - 04$	2.00	$4.6544e - 04$	2.00

Table 3.8: Spatial accuracy for the energy and the mass preserving PAVF-P method with $\Delta t = 0.01$

Δx	$L_\infty(\phi)$	order	$L_2(\phi)$	order
0.1	$4.0086e - 03$...	$5.3114e - 03$...
0.2	$9.8673e - 04$	2.00	$1.3156e - 03$	2.00
0.05	$2.4709e - 04$	2.00	$3.2688e - 04$	2.00
Δx	$L_\infty(\Psi)$	order	$L_2(\Psi)$	order
0.1	$7.7895e - 03$...	$7.4965e - 03$...
0.2	$1.9531e - 03$	2.00	$1.8626e - 03$	2.00
0.05	$4.8795e - 04$	2.00	$4.6643e - 04$	2.00

3.5.2.1 Evolution of single soliton

Now, we simulate the evolution of a single soliton. The initial conditions are taken as

$$\begin{aligned}
 \phi_0(x) &= \phi(x, 0, x_0, B, c) \\
 \psi_0(x) &= \psi(x, 0, x_0, B, c) \\
 \psi_1(x) &= \partial_t \psi(x, t, x_0, B, c)|_{t=0}
 \end{aligned} \tag{3.55}$$

We choose by choosing $c = 0.5$, $B = 0.5$. The spatial domain $x \in [-32, 32]$ is large enough so that the boundaries do not affect the solitary wave propagation. First we consider the energy preserving schemes with $\Delta x = 0.1$, $\Delta t = 0.02$. Figures 3.1 and 3.2 represents the evolution of a single solitary wave located at the position $x_0 = -5$ at $T = 0$ and $T = 20$. From the figure we see that the waves $|\phi|$ and ψ move to the right keeping their shapes and amplitudes. This shows that there is no loss of energy during the propagation. Moreover, oscillations are not observed. We conclude that all energy preserving schemes well simulate the solitary wave of the Zakharov equation. Figures 3.3 and 3.4 show the corresponding relative errors in Hamiltonian and the mass.

In order to illustrate the long-time behaviour of the four energy preserving schemes and to show the effect of the periodic boundary conditions, we perform another test. Figure 3.5 and 3.6 represent the wave profiles $|\phi^n| = |u^n + iv^n|$ and ψ^n from $t = 0$ to $t = 150$ obtained from the four energy preserving schemes AVF (3.44), PAVF (3.45), PAVF-C (3.50) and PAVF-P (3.51). We choose $\Delta x = 0.1, \Delta t = 0.01$ and $c = B = 0.5$. The initial wave is located at $x_0 = -15$. We see that all schemes produces almost same profile. The usage of the periodic boundary conditions can be seen from the figures. We see that single wave moves in the right direction, hits the

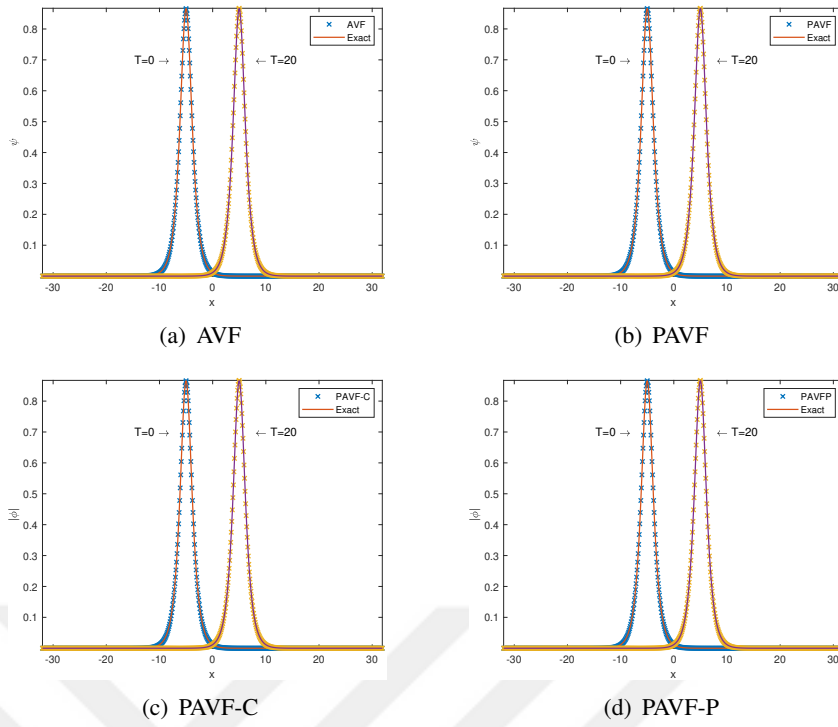


Figure 3.1: Propagation of one soliton: $|\phi(t, x)|$.

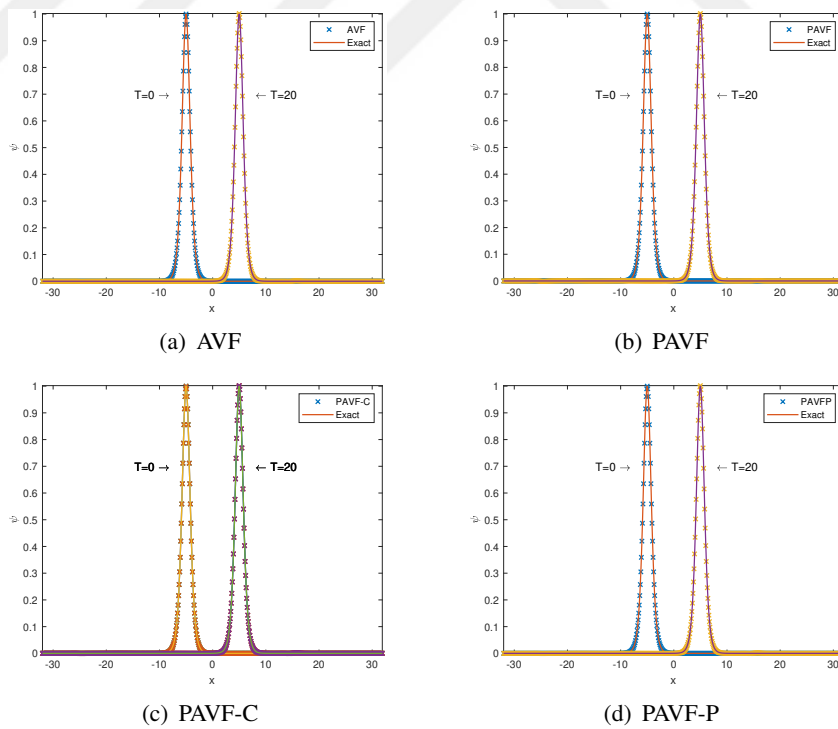


Figure 3.2: Propagation of one soliton: $\psi(t, x)$.

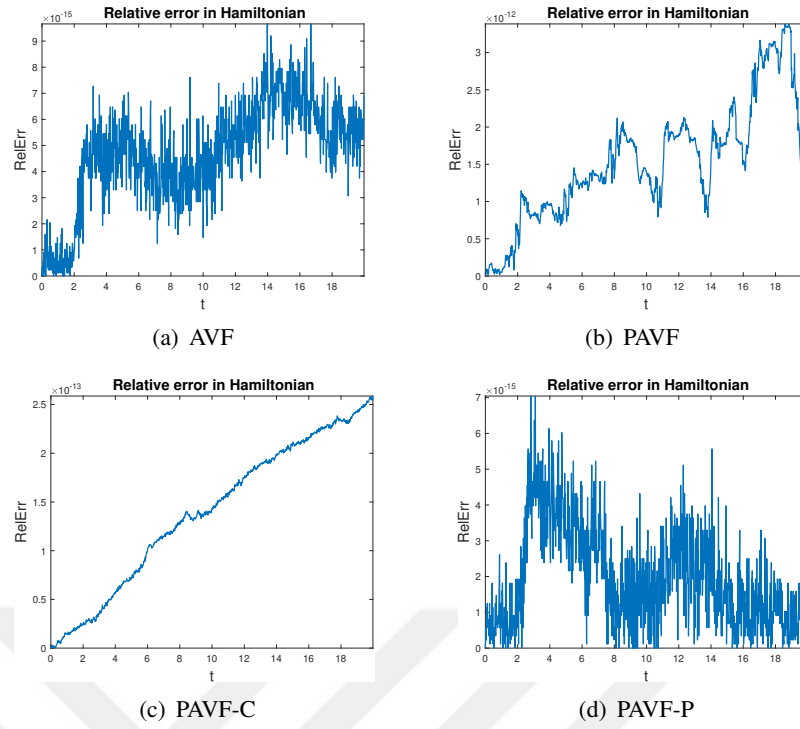


Figure 3.3: Relative Hamilton error for the propagation of one soliton: $|\phi(t, x)|$.

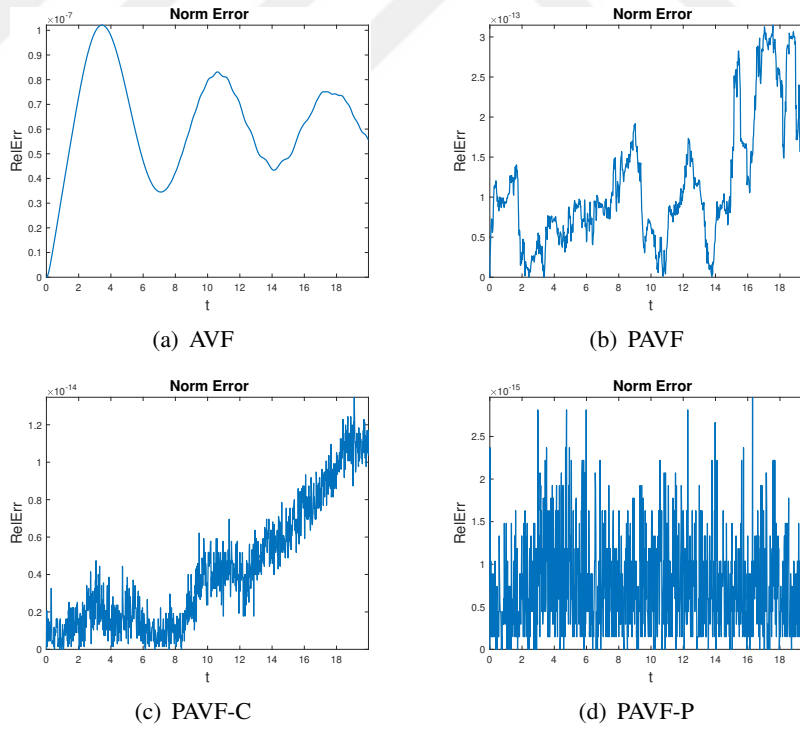


Figure 3.4: Relative norm error for the propagation of one soliton: $\psi(t, x)$.

right boundary and reappear from left due to the periodic boundary condition. Then the wave continue to move in the right direction without any changes in its shapes. This shows that all schemes well simulate the solitary wave. Figure 3.7 shows the relative energy error of the single soliton at $t \in [0, 150]$. From the figure we see that all the methods preserve the energy exactly. Figure 3.8 represents the relative mass error of the single soliton at $t \in [0, 150]$. From the figure we see that all new energy preserving schemes PAVF (3.45), PAVF-C (3.50) and PAVF-P (3.51) preserves the mass exactly up to the machine round-off error except the AVF (3.44) method which is not mass conserving. We see that relative mass error of the AVF scheme is bounded during the time evolution. From these numerical results, we conclude that, in contrast to the AVF scheme, the three partitioned AVF schemes, namely PAVF, PAVF-C and PAVF-P, have excellent preservation properties of the Zakharo equation (3.32).

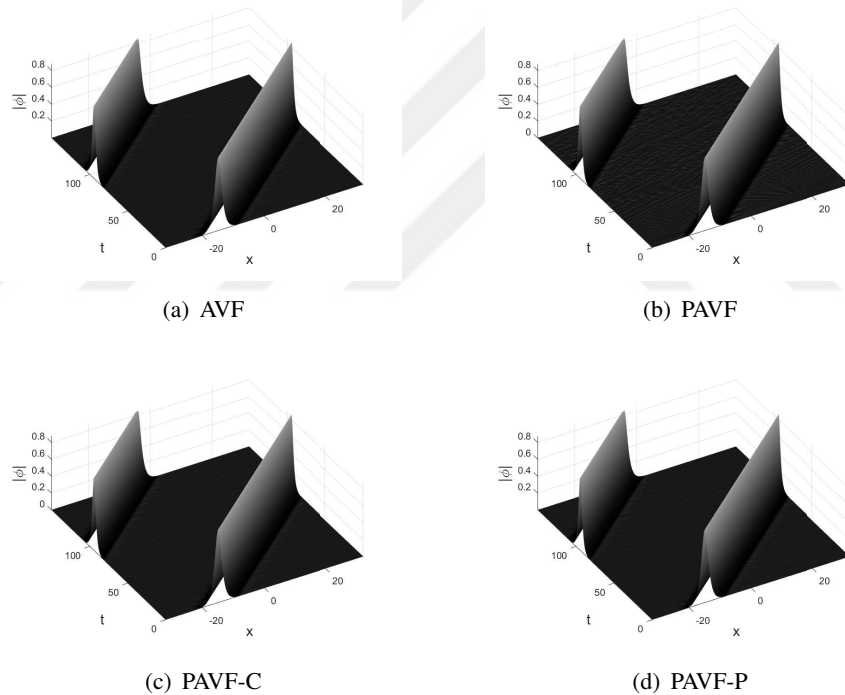


Figure 3.5: Propagation of one soliton: $|\phi(t, x)|$.

The computational cost of the four energy preserving methods with different step sizes are listed in Table 3.9. From the table we see that CPU time of the linearly implicit methods PAVF and PAVF-C methods are much less than the fully implicit methods AVF and PAVF-P. Moreover, the CPU time of the PAVF-C is much less than the twice

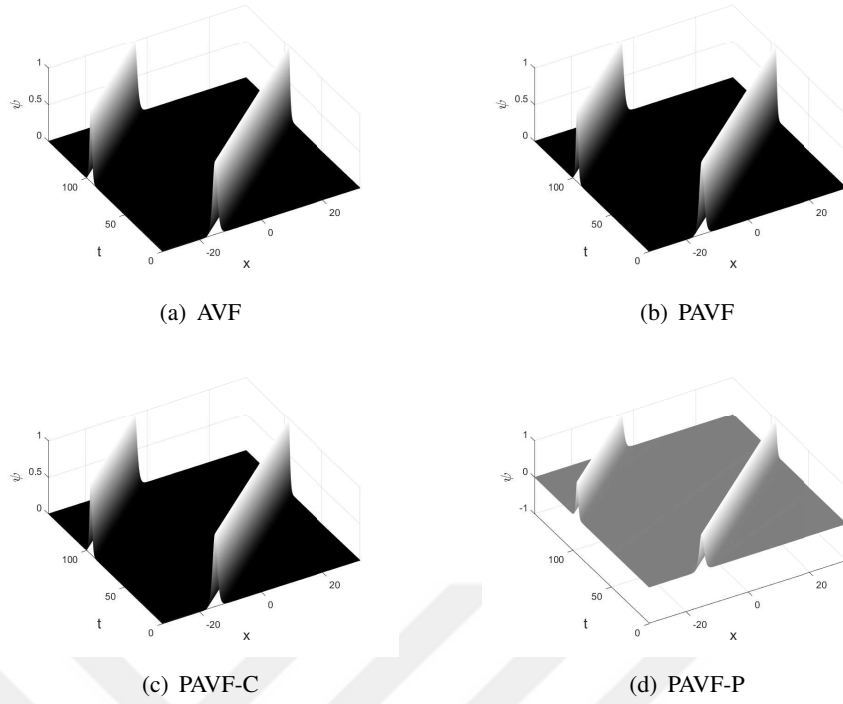


Figure 3.6: Propagation of one soliton $\psi(t, x)$.

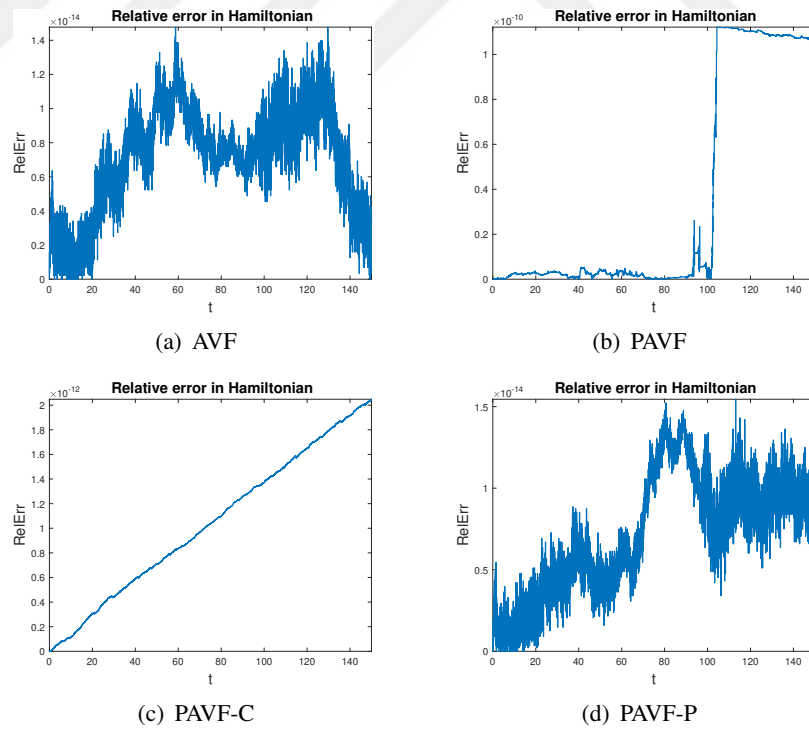


Figure 3.7: Relative Hamiltonian error for the propagation of one soliton.

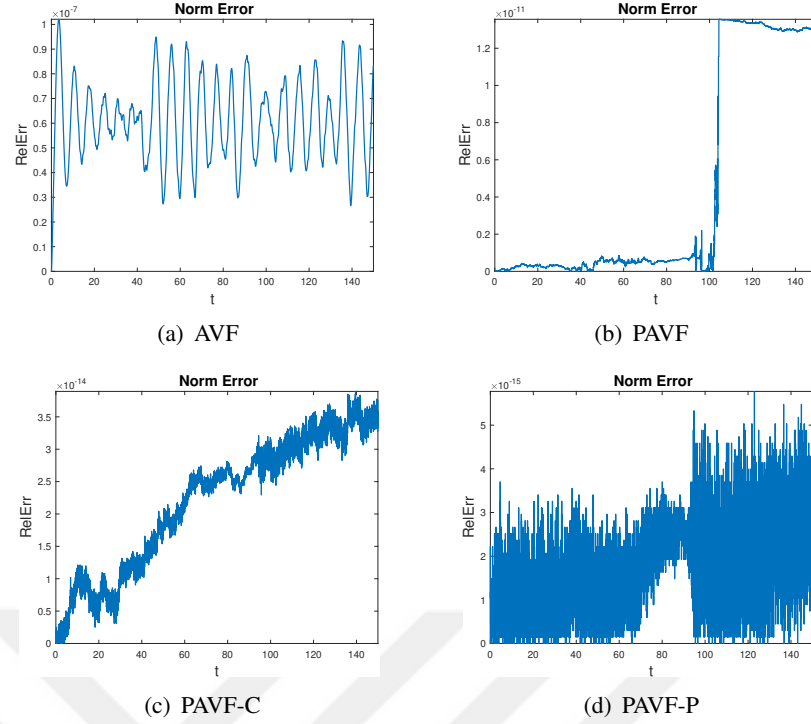


Figure 3.8: Relative norm error for the propagation of one soliton.

Table 3.9: Computational costs of one soliton solution by energy preserving schemes with $\tau = 0.01$ at $T = 1$

h	AVF	PAVF	PAVF-C	PAVF-P
1/2	3.26	0.50	0.75	3.56
1/5	25.07	1.55	2.74	26.03
1/10	159.33	7.03	13.68	156.06
1/15	426.64	16.23	35.08	367.29

of that of PAVF. Similar results are obtained in [1].

3.5.2.2 Colliding solitons

In this section, we will study the collision of two solitary waves. We consider the following initial conditions

$$\begin{aligned}
 \phi_0(x) &= \phi(x, 0, x_1, B_1, c_1) + \phi(x, 0, x_2, B_2, c_2) \\
 \psi_0(x) &= \psi(x, 0, x_1, B_1, c_1) + \psi(x, 0, x_2, B_2, c_2) \\
 \psi_1(x) &= \partial_t \psi(x, t, x_1, B_1, c_1)|_{t=0} + \partial_t \psi(x, t, x_2, B_2, c_2)|_{t=0}
 \end{aligned} \tag{3.56}$$

We set $x_1 = -x_2 = 20$, $c_1 = -c_2 = 0.5$ and $B_1 = B_2 = 0.5$. We simulate the two solitary wave within the spatial domain $x \in [-32, 32]$ and the time interval $[0, 80]$. The computations are performed with $\Delta x = 0.1$, $\Delta t = 0.02$. The initial conditions (3.56) represents two solitary waves with equal amplitude located at the spatial position $x = -20$ and $x = 20$. Figures 3.9, 3.10, 3.11 and 3.11 represents the simulation of two solitary waves obtained from the AVF (3.44), PAVF (3.45), PAVF-C (3.50) and PAVF-P (3.51) methods. From these figures we see that the solitary wave located to the position $x = -20$ is moving to the right and the wave located to the $x = 20$ is moving to the left without changing their shapes and keeping their profiles up to the collision. Then, two solitary waves collides each other. This is a head-on collision or symmetric collision. We see that the collision results the fusion of two waves. The collision results in fusion accompanied by a series of emission. After the collision, we also see that the amplitudes of the waves increase. Figures 3.5 and 3.6 exhibits the three dimensional graphes of the head-on collisions of two solitary waves. We see that the collision takes places at time around $t = 40$. Figures 3.15 represents the relative errors of energy for head-on collision. It can be observed from the graphs that the relative errors in energy are all in the scale of between 10^{-12} and 10^{-14} . These numerical results verify the present four schemes are energy-preserving methods. Figures 3.16 represents the relative errors of norm for head-on collision. From the figure, we see the errors in mass for PAVF, PAVF-C and PAVF-P methods all oscillate near zeros in the scale of at most 10^{-13} . This figure verify that, on the contrary of the AVF method, the methods PAVF, PAVF-C and PAVF-P are mass conserving methods. Obviously, the three methods PAVF, PAVF and PAVF-P all preserve the energy and mass conservation law exactly.

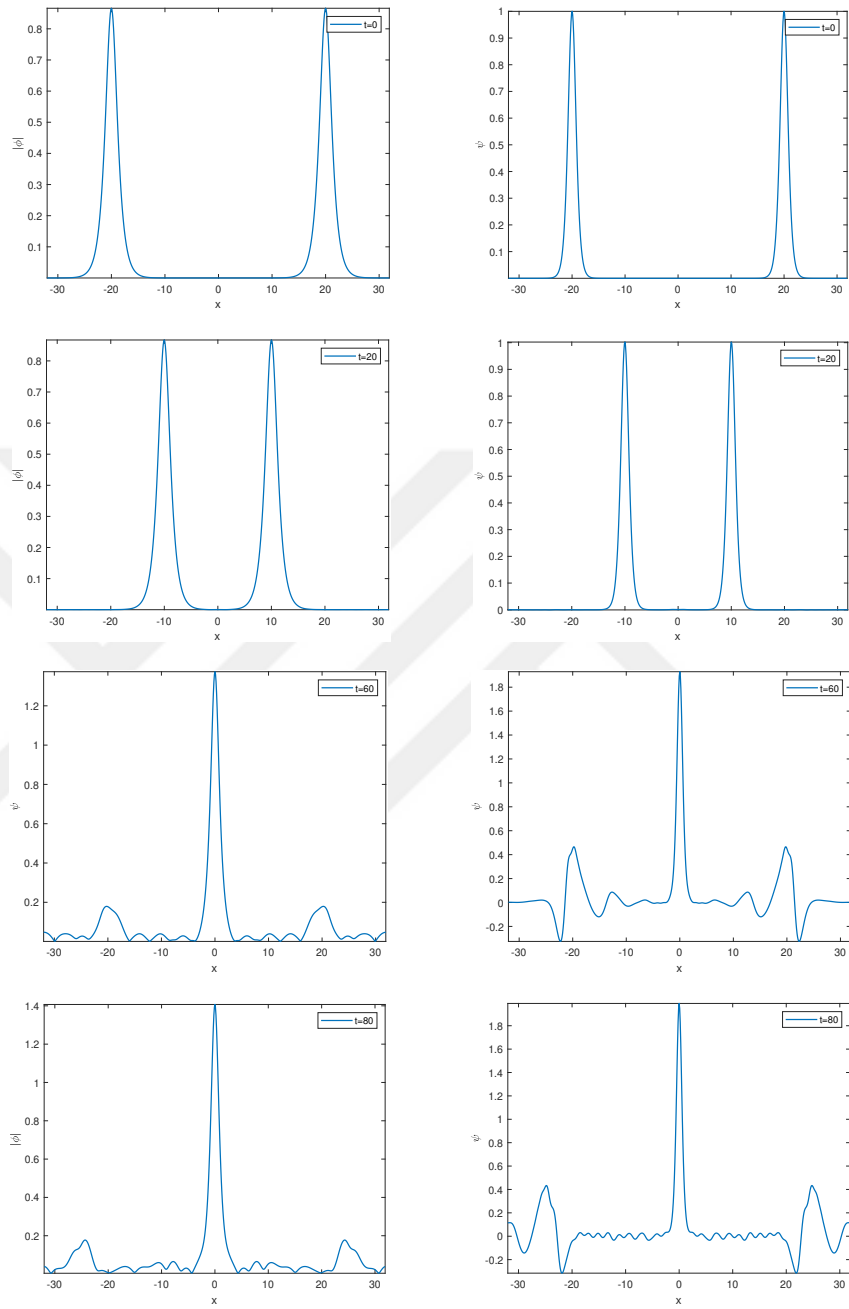


Figure 3.9: The head-on collision of two solitary waves. AVF scheme.

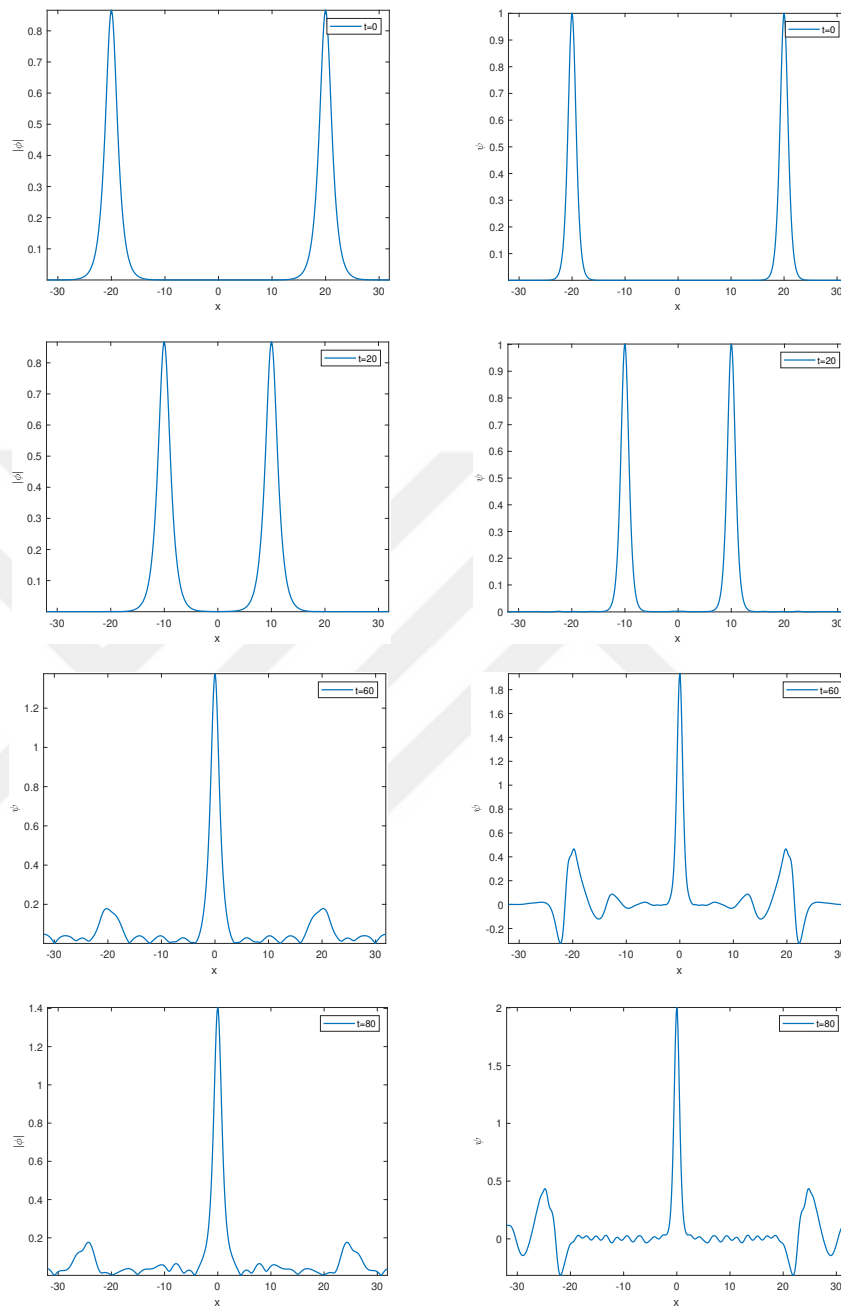


Figure 3.10: The head-on collision of two solitary waves. PAVF scheme.

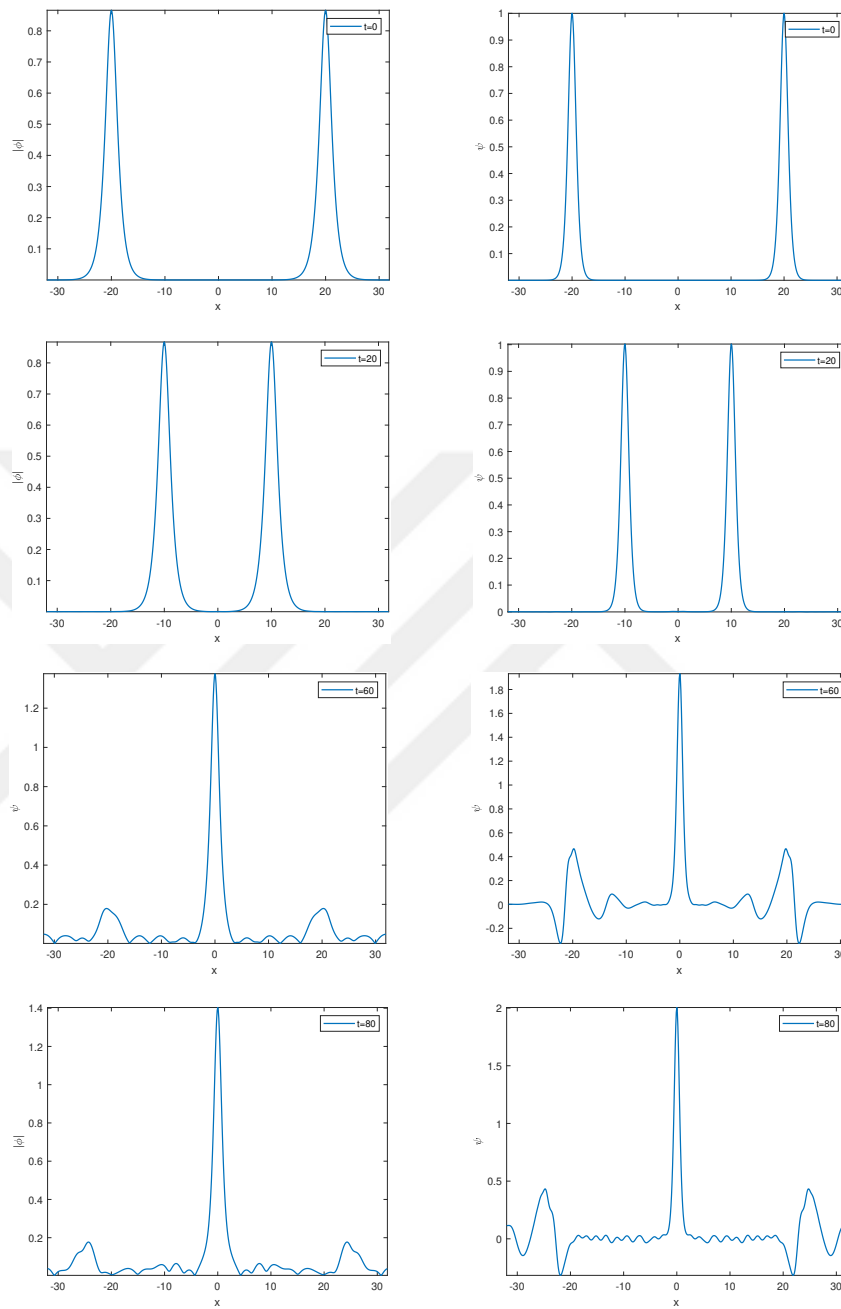


Figure 3.11: The head-on collision of two solitary waves. PAVF-C scheme.

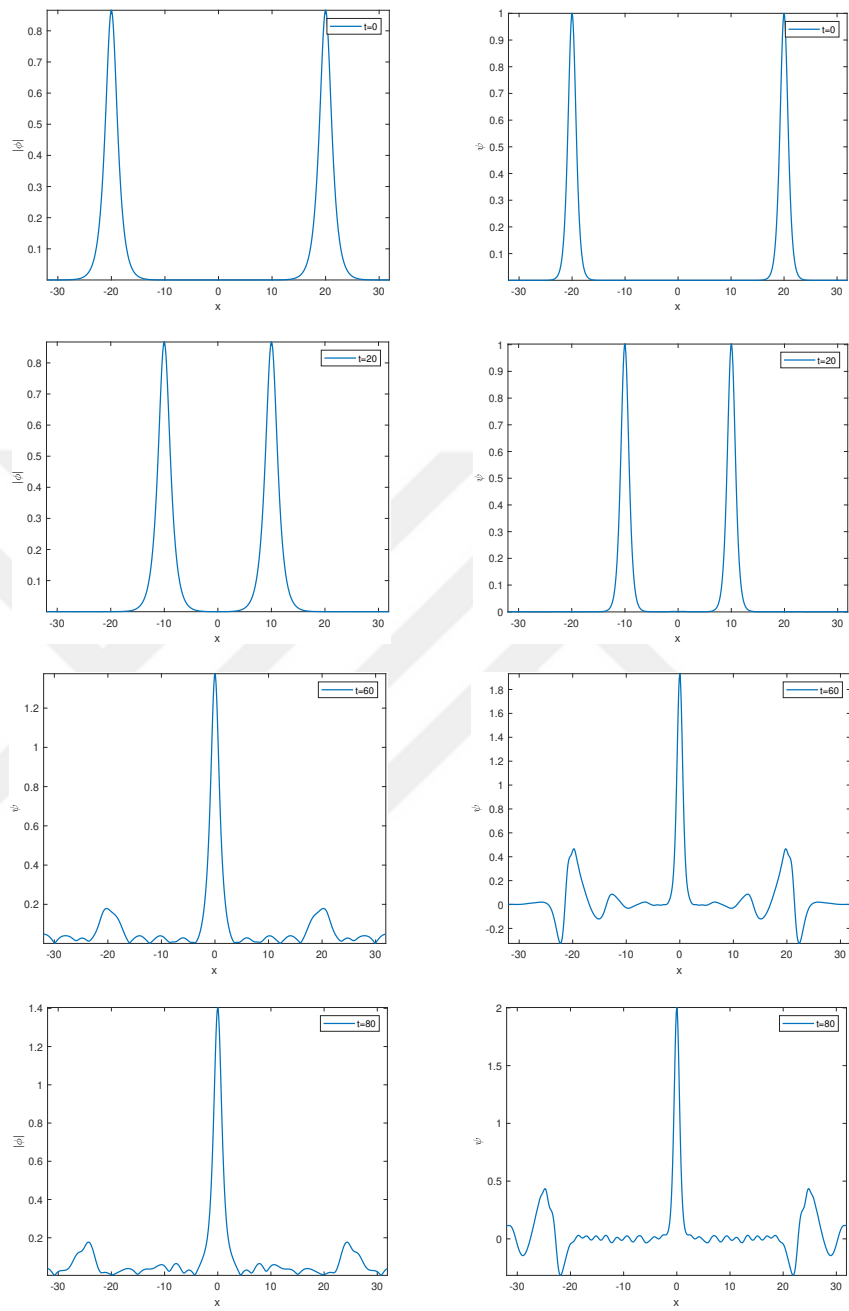
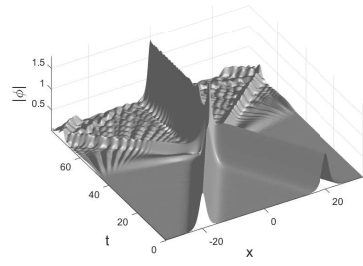
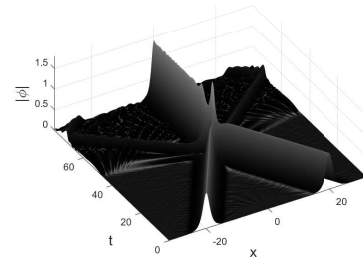


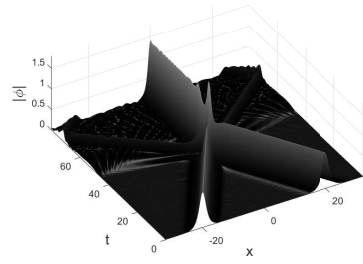
Figure 3.12: The head-on collision of two solitary waves. PAVF-P scheme.



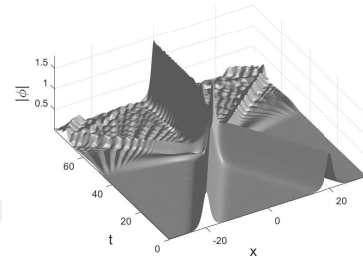
(a) AVF



(b) PAVF

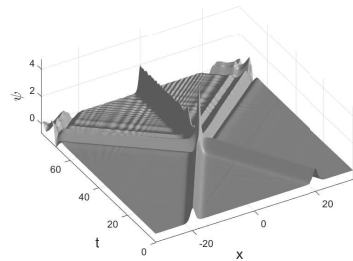


(c) PAVF-C

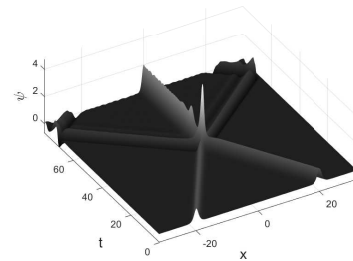


(d) PAVF-P

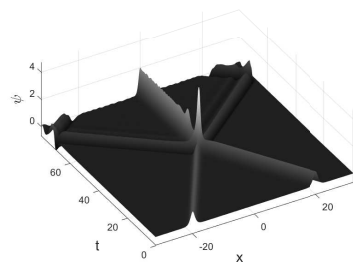
Figure 3.13: The head-on collision of two solitary waves. Profile of $|\phi(t, x)|$.



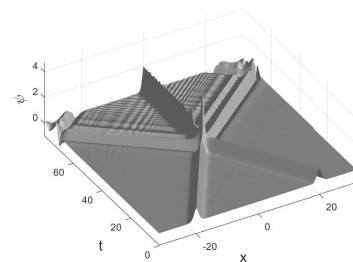
(a) AVF



(b) PAVF



(c) PAVF-C



(d) PAVF-P

Figure 3.14: The head-on collision of two solitary waves. Profile of $\psi(t, x)$.

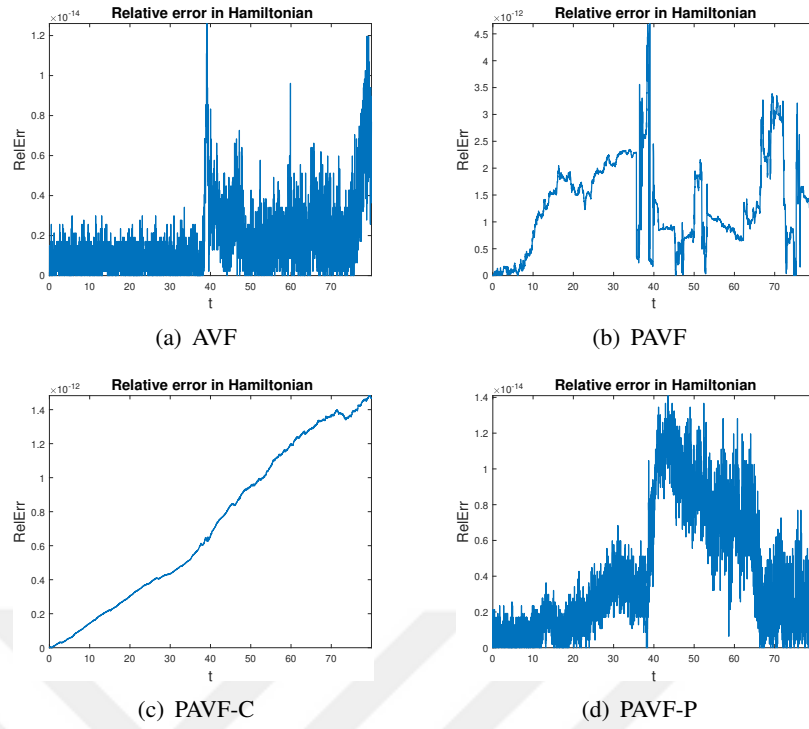


Figure 3.15: The head-on collision of two solitary waves. Relative Hamiltonian errors.

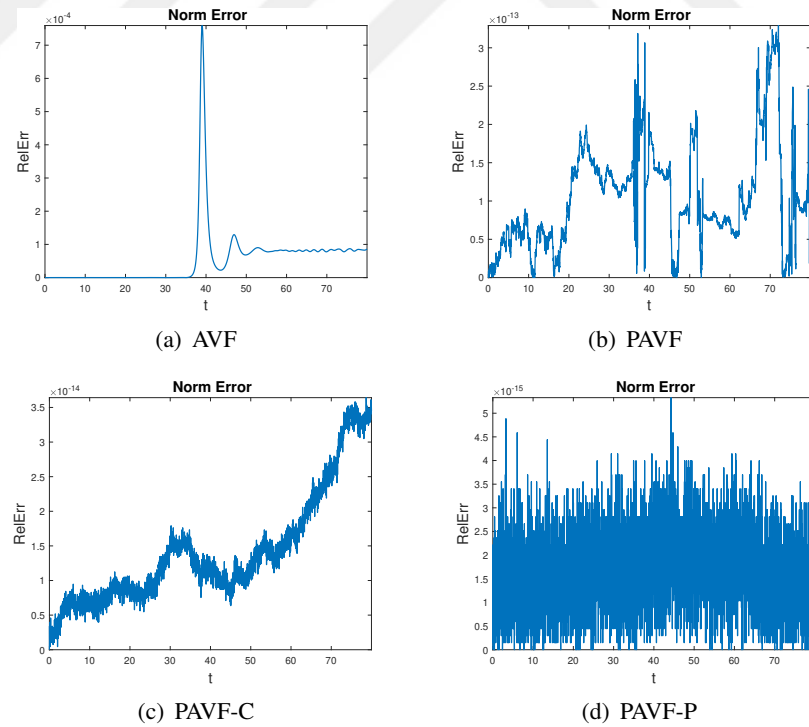


Figure 3.16: The head-on collision of two solitary waves. Relative norm errors.

CHAPTER 4

CONCLUSION

In this thesis the Average Vector Field (AVF) method and Partitioned Average Vector Field (PAVF) method are applied to Hamiltonian systems. The classic second-order AVF method is fully implicit hence leads to nonlinear algebra equation for nonlinear system. Using the adjoint method of the PAVF method, PAVF composition (PAVF-C) and PAVF plus (PAVF-P) methods are presented. Concrete schemes are applied to the Zakharov system as a model problem. Some numerical result are presented for the single and colliding solitary wave solution of the Zakharov system. Numerical results show that four schemes are energy preserving. In addition, we further show that the PAVF method preserves the mass of the Zakharov system while the classical second-order AVF method cannot. Errors of the methods are compared. We find that errors of the PACF-C scheme is less than that of PAVF scheme. Computational costs of the methods are also compared. We find that CPU times of the fully implicit methods AVF and PAVF-P methods are much larger than that of linearly implicit methods PAVF and PAVF-C. Therefore, we have concluded that the linearly implicit methods PAVF and PAVF-C method are convenient energy preserving and mass preserving method for numerical solution of the Zakharov equation.

REFERENCES

- [1] W. Cai, H. Li, Y. Wang, "Partitioned average vector field methods." *Journal of Computational Physics*, vol. 370, 25-42, 2018.
- [2] Z. Ge, "Equivariant symplectic difference schemes and generating functions." *Phys. D*, 1991, pp. 376-386.
- [3] E. Celledoni, V. Grimm, R.I. McLachlan, D.I. McLaren, D. O'Neale, B. Owren, G.R.W. Quispel, "Preserving energy rep. dissipation in numerical PDEs using Average Vector Field" method." *Journal of Computational Physics*, vol. 231, pp. 6770-6789, 2012.
- [4] G.R.W. Quispel and D.I. McLaren, "A new class of energy-preserving numerical integration methods." *J. Phys. A: Math. Theo.*, vol. 41, p. 045206, 2008.
- [5] H. Li, Y. Wang, "A sixth order average vector field method." *Journal of Computational Mathematics*, vol.34(5), pp. 451-470, 2016.
- [6] E. Hairer, C. Lubich, G. Wanner, *Geometric Numerical Integration: Structure-Preserving Algorithms for Ordinary Differential Equations*, 2nd edition, Berlin: Springer-Verlag, 2006.
- [7] L. Brugnano, F. Iavernaro, *Line Integral Methods for Conservative Problems*. Chapman and Hall/CRC, 2019.
- [8] S. Blanes, F. Casas, *A Concise Introduction to Geometric Numerical Integration*, New York: CRC Press, 2016.
- [9] J. Wang, "Multisymplectic numerical method for the Zakharov system." *Comp. Phys. Commun.*, vol.180, 2009, pp. 1063-1071.
- [10] H. Li, Y. Wang, "An averaged vector field Legendre spectral element method for the nonlinear Schrödinger equation." *Int. J. Comp. Math.*, vol. 94(6), 2017, pp. 1196-1218.
- [11] E.E. Zotos, "Classifying orbits in the classical Hénon–Heiles Hamiltonian system." *Nonlinear Dyn.* vol.79, 2015, pp.1665–1677.
- [12] J.L. Hong, S.S. Jiang, C. Li, "Explicit multi-symplectic methods for Klein–Gordon–Schrödinger equations." *J. Comput. Phys.* vol.228, 2009, pp.3517–3532.
- [13] J.J. Zhang, L.H. Kong, "New energy-preserving schemes for Klein–Gordon–Schrödinger equations." *Appl. Math. Model.*, vol.40, 2016, pp.6969–6982.

- [14] E. Celledoni, R.I. McLachlan, D.I. McLaren, B. Owren, G.R.W. Quispel and W.M. Wright, "Energy-preserving Runge-Kutta methods." *Math. Model. Numer. Anal.*, vol.43, 2009, pp.645-649.
- [15] P. Chartier, E. Faou, A. Murua, "An algebraic approach to invariant preserving integrators: the case of quadratic and Hamiltonian invariants." *Numer. Math.*, vol.103, 2006, pp.575-590.
- [16] E. Hairer, "Energy-preserving variant of collocation methods." *ESCM*, vol.5,(1-2), 2010, pp.73-84.
- [17] M.T. Heath, *Scientific Computing: An Introductory Survey*, Philadelphia:SIAM, 2018.
- [18] O. Gonzales, "Time integration and discrete Hamiltonian systems." *J. Nonlinear Sci.* vol.6, 1996, pp.449-467.
- [19] T. Itoh, K. Abe, "Hamiltonian-Conserving Discrete Canonical Equations Based on Variational Difference Quotients." *J. Comp. Phys.*, vol.77, 1988, pp.85-102.
- [20] A. Harten, P.D. Lax, B. van Leer, "On upstream differencing and Godunov-type schemes for hyperbolic conservation law." *SIAM Review*, vol.25, 1983, pp.35-61.
- [21] H. Baohui, L. Dong, "Energy-preserving time high-order AVF compact finite difference schemes for nonlinear wave equations with variable coefficients." *J. Comp. Phys.*, vol.421, 2020, p.109738.
- [22] E. Kit, L. Shemer, "Spatial versions of the Zakharov and Dysthe evolution equations for deepwater gravity waves." *J. Fluid Mech.*, vol.450, 2002, pp.201-205.
- [23] M.V. Goldman, "Strong turbulence of plasma waves." *Rev. Modern Phys.*, vol. 56(4), 1984, pp.709-735.
- [24] D. Anderson, "Variational approach to nonlinear pulse propagation in optical fibers." *Phys. Rev. A*, vol.27(6), 1983, pp.3135-3145.
- [25] A. Montina, U. Bortolozzo, S. Residori, and F. T. Arecchi, "Non-Gaussian statistics and extreme waves in a nonlinear optical cavity." *Phys. Rev. Lett.*, vol.103, 2009, p. 173901.
- [26] D.R. Solli, C. Ropers, P. Koonath, B. Jalali, "Optical rogue waves." *Nature*, vol.450, 2007, pp.1054-1057.
- [27] R. Hohmann, U. Kuhl, H.J. Stockmann, L. Kaplan, E. J. Heller, "Freak waves in the linear regime: A microwave study." *Phys. Rev. Lett.*, vol.104, 2010, p.093901.
- [28] A.N. Ganshin, V.B. Efimov, G. V. Kolmakov, L. P. Mezhev-Deglin, P. V. E. McClintock, "Observation of an inverse energy cascade in developed acoustic turbulence in superfluid helium." *Phys. Rev. Lett.*, vol.101, 2008, p.065303.
- [29] W.M. Moslem, "Langmuir rogue waves in electron-positron plasmas." *Phys. Plasmas*, vol.18, 2011, p.032301.

- [30] H. Bailung, S.K. Sharma, Y. Nakamura, "Observation of Peregrine solitons in a multicomponent plasma with negative ions." *Phys. Rev. Lett.*, vol.107, 2011, p.255005.
- [31] B. Hafizi, "Nonlinear evolution equations, recurrence and stochasticity." *Phys. Fluids* vol.24(10), 1981, pp.1791–1798.
- [32] K. Feng, "Difference schemes for Hamiltonian formalism and symplectic geometry." *J. Comput. Math.*, vol. 4, 1986, pp.279–289.
- [33] K. Feng, M.Z. Qin, *Symplectic Geometric Algorithms for Hamiltonian Systems*. Berlin:Springer-Verlag, 2010.
- [34] E. Hairer, S.P. Norsett, and G. Wanner, *Solving Ordinary Differential Equations I, Nonstiff Problems*, 2nd ed., Berlin:Springer-Verlag, 1993.
- [35] A. Iserles, *A First Course in the Numerical Analysis of Differential Equations*, 2nd ed., Cambridge:Cambridge University Press, 2008.
- [36] J.M. Sanz-Serna, "Runge-Kutta schemes for Hamiltonian systems.", *BIT*, vol.28, 1988, pp.877–883.
- [37] R. McLachlan, "Symplectic integration of Hamiltonian wave equations." *Numer. Math.*, vol.66, 1993, pp.465–492.
- [38] T.J. Bridges, S. Reich, "Multi-symplectic spectral discretizations for the Zakharov–Kuznetsov and shallow water equations." *Physica D*, vol. 152, 2001, pp.491–504.
- [39] J.B. Chen, M.Z. Qin, "Multi-symplectic fourier pseudospectral method for the nonlinear Schrödinger equation." *Electron. Trans. Numer. Anal.*, vol.12 2001, pp.193–204.
- [40] B. Fornberg, *A Practical Guide to Pseudospectral Methods*, Cambridge:Cambridge University Press, 1996.
- [41] L.C. Jan, "Improving the accuracy of the AVF method." *J. Comput. Math.*, vol.259, 2014, pp.233-243.
- [42] C. Akkoyunlu, B. Karasözen, "Average Vector Field Splitting Method for Nonlinear Schrödinger Equation," in *Proc. Chaos and Complex Systems*, 2013, pp 245-251.
- [43] W. Yu, X. Wu, "General local energy-preserving integrators for solving multi-symplectic Hamiltonian PDEs." *Journal of Computational Physics*, vol.301, 2015, pp.141–166.
- [44] B.N. Ryland, R.I. McLachlan, J.Frank, "On the multisymplecticity of partitioned Runge Kutta and splitting methods." *J. Com. Math.* vol.84(6), 2007, pp.847-869.
- [45] O. Gonzalez, "Time integration and discrete Hamiltonian systems." *J. Nonlinear Sci.* vol.6, 1996, pp.449–467.
- [46] T. Matsuo, "High-order schemes for conservative or dissipative systems." *J. Comput. Appl. Math.*, vol.152, 2003, pp.305–317.

- [47] L. Brugnano, F. Iavernaro, and D. Trigiante, "Hamiltonian boundary value methods(Energy preserving discrete line integral methods." *J. Numer. Anal. Ind. Appl. Math.*, vol.5, 2010, pp.17-37.
- [48] F. Iavernaro, D. Trigiante, "High-order symmetric schemes for the energy conservation of polynomial Hamiltonian problems." *J. Numer. Anal. Ind. Appl. Math.*, vol.4, 2009, pp.87–101.
- [49] G.R.W. Quispel, D.I. McLaren, "A new class of energy-preserving numerical integration methods." *J. Phys. A, Math. Theor.*, vol.41, 2008, p.045206.
- [50] R.I. McLachlan, G.R.W. Quispel, N. Robidoux, "Geometric integration using discrete gradient." *Phil. Trans. R. Soc.* vol.357, 1999, pp.1021–1045.
- [51] C.L. Jiang, J.Q. Sun, "A high order energy preserving scheme for the strongly coupled nonlinear Schrodinger system." *Chin. Phys. B*, vol.23(5), 2014, p.050202
- [52] K. Feng, "Difference schemes for Hamiltonian formalism and symplectic geometry." *J. Comput. Math.*, vol.4, 1986, pp. 279–289.
- [53] K. Feng and M.Z. Qin, *Symplectic Geometric Algorithms for Hamiltonian Systems*, Berlin:Springer-Verlag, 2010.
- [54] E. Celledoni, R.I. McLachlan, D.I. McLaren, B. Owren, G.R.W. Quispel, and W.M. Wright. "Energy-preserving Runge-Kutta methods.", *M2AN.*, vol.43, 2009, pp.645–649.
- [55] J. Chen, M, Qin, F. Tang, "Symplectic and Multi-Symplectic Methods for the Nonlinear Schrodinger Equation." *Computers and Mathematics with Applications*, vol.43, 2002, pp.1095-1106.
- [56] A. Aydin, B. Karasozen, "Symplectic and multisymplectic Lobattot methods for the "good" Bouissinesq equation." *J. Math. Phys.*, vol.49, 2008, p.083509.
- [57] R. Glassery, "Convergence of an energy-preserving scheme for the Zakharov equations in one space dimension." *Math. Comput.*, vol. 58, 1992, pp.83-102.